



Assessing the water balance of the Upper Rhine Graben hydrosystem

Charlotte Thierion, Laurent Longuevergne, Florence Habets, Emmanuel Ledoux, Philippe Ackerer, Samer Majdalani, Etienne Leblois, Simon Lecluse, Eric Martin, Solen Queguiner, et al.

► To cite this version:

Charlotte Thierion, Laurent Longuevergne, Florence Habets, Emmanuel Ledoux, Philippe Ackerer, et al.. Assessing the water balance of the Upper Rhine Graben hydrosystem. *Journal of Hydrology*, 2012, 424, pp.68-83. 10.1016/J.JHYDROL.2011.12.028 . hal-00708218

HAL Id: hal-00708218

<https://hal.science/hal-00708218>

Submitted on 14 Jun 2012

HAL is a multi-disciplinary open access archive for the deposit and dissemination of scientific research documents, whether they are published or not. The documents may come from teaching and research institutions in France or abroad, or from public or private research centers.

L'archive ouverte pluridisciplinaire **HAL**, est destinée au dépôt et à la diffusion de documents scientifiques de niveau recherche, publiés ou non, émanant des établissements d'enseignement et de recherche français ou étrangers, des laboratoires publics ou privés.

Assessing the water balance of the Upper Rhine Graben hydrosystem

Charlotte Thierion^{a,*}, Laurent Longuevergne^b, Florence Habets^a, Emmanuel Ledoux^c, Philippe Ackerer^d, Samer Majdalani^e, Etienne Leblois^f, Simon Lecluse^d, Eric Martin^g, Solen Queguiner^g, Pascal Viennot^c

a. Sisyphe, UPMC, CNRS, Mines-Paristech, Fontainebleau, France

b. Geosciences, Université Rennes 1, CNRS, Rennes, France

c. Centre de Géosciences, Mines-Paristech, Fontainebleau, France

d. LHYGES, Université de Strasbourg, CNRS, Strasbourg, France

e. HydroSciences, Université Montpellier 2, CNRS, Montpellier, France

f. CEMAGREF, Lyon, France

g. CNRM, Météo-France, CNRS, Toulouse, France

*Corresponding author: email: charlotte.thierion@mines-paristech.fr

Tel : +33164694960 – Fax : +33164694703

Abstract

The Upper Rhine alluvial aquifer is an important transboundary water resource. However, as in many alluvial systems, the aquifer inflows and outflows are not precisely known, due to the difficulty in estimating the river infiltration flux and the boundary subsurface flow. To provide a thorough representation of the aquifer system, a coupled surface-subsurface model was applied on the whole aquifer basin, and several parameter sets were tested to investigate the uncertainty due to poorly known parameters (e.g. aquifer transmissivity computed by an inverse model, river bed characteristics). Twelve simulations were run and analysed using standard statistical criteria, as well as a more advanced statistical method, the Karhunen

Loève Transform (KLT). This analysis showed that although the model performs reasonably well, some piezometric levels underestimations persist in the south of the basin. An accurate representation of the aquifer behaviour requires taking into account river infiltration and the functioning of irrigation canals in the Hardt area. It also appeared that increasing the maximum river infiltration flow leads to altered results.

River infiltration to the aquifer was estimated to represent about 80 % of the aquifer inflows with a mean annual value around $115 \pm 16.5 \text{ m}^3/\text{s}$, therefore with an uncertainty of 14 %. This quantity is larger than estimated in previous studies, but also in agreement with some results obtained during low water periods. This important conclusion highlights the vulnerability of the Upper Rhine Graben aquifer to pollution from the rivers and to climate change since it is highly probable that the rivers' regime from the neighbouring mountain ranges will be affected by a reduced snow cover.

Keywords: groundwater-surface water relations; groundwater recharge/water budget; Upper Rhine alluvial aquifer; hydrogeological model parameters sensitivity.

1 Introduction

Alluvial hydrosystems have been recognised as important water resources but also very vulnerable systems to pollution or change in water availability (Allen et al., 2004). Knowledge of the different components of the water balance is therefore of significant importance to optimize water management and/or to estimate the impacts of anthropogenic activities or climate changes. These water balance components are difficult to measure, as the observations of water fluxes provide only local information (Sanford 2002, Kalbus et al., 2006). Thus there is a need to assess these fluxes by modelling, as they are linked to the boundary conditions, the sink/source terms and the hydrodynamic parameters, which are mostly unknown and estimated through model calibration. Model calibration leads to non-

unique solutions and therefore, the evaluation of some components of the water balance is uncertain (Konikow and Bredehoeft 1992, Beven 2006).

The components of the water balance for unconfined groundwater are recharge due to precipitations, exchanges with surface water, in/out-flows through the boundaries (either prescribed heads or prescribed fluxes), storage in the aquifer, and water uptake by pumping wells. Recharge and surface-groundwater interactions constitute key processes in the behaviour and the evolution of these systems (Sanford, 2002, Woessner, 2000, Sophocleous, 2002). These fluxes can be estimated by fully coupled surface-subsurface models including the unsaturated zone such as ParFlow (Kollet and Maxwell, 2006), Hydrogeosphere (Therrien et al. 2007), and CATHY (Camporese et al., 2008) among others. However, applications of these fully coupled models are generally limited to small areas. For larger systems, coupled surface-subsurface models are usually simplified (Hu et al. 2007, Rushton 2007) and the recharge is estimated separately using simplified hydrological models based on 1D Richards equation (e.g. MIKE SHE, Reefsgard 1997) or more conceptual schemes (e.g. MARTHE, Noyer and Elsass 2006).

This work aims at estimating the different components of the water balance and its associated uncertainties for the Upper Rhine aquifer. The studied hydrosystem is one of the most important water resources in Western Europe, and several regional scale models were previously developed, as for example in the LIFE project in 1996 (LfU 1996, LfU 2005), and in the INTERREG project Monit (LUBW 2006) focusing on nitrate contamination of groundwater. These two studies led to different findings about aquifer recharge: river infiltration was found to be the main recharge component in LIFE, whereas in Monit it was effective rainfall. However, these discrepancies may be linked to the fact that the models were limited to the alluvial plain, and used simple methods to assess the subsurface flows from the Vosges and the Black Forest surrounding mountains.

In the present work a modelling of the whole Rhine basin between Basel and Lauterbourg is performed (figure 1). This enables to better constrain the lateral water inputs to the aquifer, and thus, to have a homogenous representation of the whole Upper Rhine graben basin. Moreover it allows assessing the impacts of climate change on the hydrosystem, which could lead to altered conditions over the mountainous catchments.

The Upper Rhine alluvial aquifer groundwater dynamics is modelled using different assumptions and calibration methods based on trial and errors or inverse approach. The use of several likely parameter values for a given model leads to different likely water balances and provides an estimate of the associated uncertainty. Since several possible calibrated models are obtained, we associated classic statistical criteria (average error, Nash criteria) with a more advanced statistical method, the Karhunen Loève transform (KLT) to evaluate the model performance (Wilks, 1995, Longuevergne et al., 2007). The KLT allows the decomposition of piezometric time series into several independent temporal vectors, corresponding to the main influential processes. This gives a different insight into the performances of the simulations, focused on the representation of the main influential processes over the piezometric head temporal evolution, and helps in discriminating and quantifying the model ability to represent these processes. Using the results of this analysis, the aquifer water budget and recharge components are assessed, as well as the uncertainty in their computation.

This article is organised as follows: first, the characteristics of the basin are presented. Then, the models used in this work are described (section 3), and the calibration of the surface water budget is presented (section 4). In section 5, the different parameter sets are presented, and the sensitivity of model results is analysed using the classic statistical criteria and the Karhunen Loève transform. Eventually, section 6 presents the estimation of the aquifer water budget and stock variations and the uncertainty on the recharge/discharge fluxes.

2. Basin characteristics

Figure 1 : a) Situation of the basin and topography with main rivers and gauging stations used for model calibration; b) Mean annual precipitation in mm/yr computed on the period 1983-2006 as estimated by the SAFRAN analysis (cf section 2.2).

2.1 Geographical and geological setting

The Upper Rhine graben hydrosystem, situated at the French-German border (Figure 1), is composed of three units: i) a tectonic graben containing Secondary to Tertiary sediments, several kilometres thick (Figure 2) and forming the substratum of the Rhine alluvial plain (Illies, 1972), ii) the graben shoulders with much older materials such as crystalline, metamorphic and ancient sedimentary rocks constituting the Black Forest mountains in the East and the Vosges mountains in the West, and iii) the Sundgau hills in the South, formed by marly Oligocene substratum of the Quaternary sediments which was relatively less subsided than in the rest of the graben during the continental rifting.

The graben contains Tertiary marls and clays, covered by Quaternary alluvium deposited by the Rhine River and forming the studied alluvial aquifer (cf. figure 2) (Duprat et al., 1979, Bauer et al. 2005). The hydrographic network is very dense in the plain, due to the presence of many groundwater-fed streams, allowing significant exchange of water between rivers and the aquifer (Schmitt, 2001).

Figure 2 : Geological cross section of the Rhine Graben, showing the sediment succession in the plain and relative thickness (modified from Illies (1972))

The main Rhine's tributary in this part of its basin, the Ill River (figure 1), has its source in the Sundgau, while some small rivers having their sources in the same area fully infiltrate towards the aquifer. The other most important rivers have their source in the Vosges and Black Forest mountains West and East of the plain.

The material of the Rhine alluvial aquifer is mainly coarse quaternary gravels and sands with good hydrogeological properties. The hydraulic conductivities are in the order of $10^{-4} - 10^{-3}$ m/s (Duprat et al., 1979; LfU, 1996; LUBW, 2006b). On the other hand the rocks forming the mountains are rather impervious material containing only local aquifer formations of small extension. The alluvial aquifer thickness reaches more than 200 m in its centre, East of Colmar (LUBW, 2006). Mineral composition and thus structure and texture of the sediments deposited by the Rhine River are marked by their Alpine origin, whereas towards the edges of the graben, Vosgian and Black Forest rivers have deposited alluvial material having different hydrogeological properties. These elements contribute to the heterogeneity of the aquifer material, which in turn impacts the geometry of the river-aquifer interactions.

The aquifer substratum consists of the Oligocene marls considered impervious. The groundwater flows from South to North and is closer to the surface in its northern part. Water table depths range from 0 to 20 m (Hardt area), and groundwater fed wetlands are present in the middle and the northern parts of the plain.

2.2 Climatic conditions

Precipitations show large contrasts over the basin, with annual values ranging from 550 mm/year in the plain, to more than 2000 mm/year in the Vosges and Black Forest mountains (Figure 1). Snowfalls account for around 3 % of total precipitations in the plain, and up to 37 % at the mountains tops. Thus snow accumulation and melting are important processes for the dynamics of river flows in these catchments. Moreover potential evapotranspiration, computed with Penman formula on the 1983-2006 time period, is weaker on the mountains

tops (around 600 mm/year) than in the plain (around 800 mm/year). As a consequence the rivers flowing from the mountainous catchments carry an important proportion of the water involved in the hydrosystem budget and play a crucial role in the recharge of the Rhine alluvial aquifer.

Daily precipitations and potential evapotranspiration (PET) for the modelling are provided by the SAFRAN analysis performed by Météo France, based on the definition of climatologically homogeneous zones and on altitudinal variation of the meteorological variables (Quintana-Seguí et al 2008, Vidal et al., 2010). They are used here at a daily time step from 1985 to 2003, which is about the period of time used in the previous Monit project (LUBW 2006). For the present study the SAFRAN analysis that is usually provided on a regular grid of 8x8 km² was projected over a specific grid with cells varying from 1 to 8 km size in order to better account for the topographic gradient of precipitation (Figure 1).

2.3 Available data

Daily river discharges are observed in about 20 to 30 river gauges within the studied area, depending on the time period. These gauging stations are managed mainly by the DREAL-Alsace (Direction Régionale de l'Environnement, de l'Aménagement et du Logement in Alsace) on the French side, and by the LUBW-Baden-Württemberg (Landesanstalt für Umwelt, Messungen und Naturschutz in Baden-Württemberg) on the German side. Piezometric levels data consist in numerous observation wells (more than 200 points) sampled weekly, only a few of them having daily data. These observation wells are managed mainly by the APRONA (Association pour la PROtection de la Nappe d'Alsace) on the French side and by the LUBW on the German side.

Seasonal piezometric levels fluctuations are generally limited to one meter or less, except in the South and near the Eastern and Western borders where the water table is deeper. No long term tendency appears for the piezometric levels over the simulated period, from 1985 to

2003. Nevertheless piezometric levels are rather low between 1990 and 1995, and rather high between 2000 and 2003. The same holds true for the mountain rivers discharges (cf. figure 7).

Land use is characterized by large agricultural areas in the plain, with extensive cultures of cereals (some of them being irrigated), vineyards in the piedmont, whereas the mountains are largely covered by coniferous and deciduous forests (Figure 3). Agricultural lands cover approximately 40 %, and forests 45 % of the basin. Artificial areas represent almost 10 % of the area, which is densely populated with more than 200 inhabitants/km². The main cities are Basel, Colmar, Mulhouse and Freiburg in the South, Strasbourg in the North. Important water withdrawals, around $3.6 \cdot 10^8$ m³/yr, are located close to these cities for drinking and industrial purpose. Irrigated agricultural areas represent around 6 % of the region, mostly in the Southern central part of the plain.

3. Models presentation

Two different models were used: one classical hydrogeological model (MODCOU, Ledoux et al., 1989), and one hydrogeological model including an inversion of the model parameters capacity (HPP-INV, Majdalani and Ackerer, 2010).

In this section, the models are presented briefly, with a special focus on MODCOU which is mainly used in this study.

3.1. MODCOU

MODCOU is a spatially distributed coupled hydrogeological modelling tool that was already used in several large basins in France (Golaz-Cavazzi et al., 2001, Ledoux et al., 2007, Korkmaz et al., 2009).

It is built up on several interconnected modules. The first one is dedicated to the estimation of the surface water budget computed with a simple reservoir scheme, the production functions

(Figure 4). Inputs to this conceptual model are the daily precipitation and potential evapotranspiration (PET) data on a spatial grid. Outputs are actual evapotranspiration (AET), infiltration and runoff on each grid cell and at a daily time step. More details on the production functions are given in the next section where the calibration of the surface water budget is presented.

The direct infiltration of water from effective rainfall through the unsaturated zone is simulated with a Nash cascade (Philippe et al., 2010).

The aquifer representation is based on a square grid discretization, with a finite differences resolution of the diffusivity equation. The rivers flows are simulated according to a Muskingum scheme (David et al., 2011).

There are two kinds of interactions between the surface and the groundwater: 1) the aquifer can be drained where piezometric level reaches the soil level, and 2) drainage or infiltration of water towards the aquifer can occur on river cells. Owing to the major role of the river-aquifer interactions on the Upper Rhine Graben aquifer, the description of these processes in MODCOU is further detailed here.

On river cells, the river-aquifer exchange flow is proportional to the head difference between the river and the aquifer, to permeability and width of the riverbed, and inversely proportional to its thickness. As these characteristics of the river bed are mostly unknown, they are integrated in two parameters called the transfer coefficient (T_p), for the case when the aquifer and the river are connected, and the maximum river infiltration flow (Q_{lim}) for the disconnected case (Rushton 2007). The exchange flow is therefore computed as follows:

$$Q_{exch} = \max\left(T_p(H_{gw} - H_{riv}); -Q_{lim}; -Q_{dis}\right), \quad (1)$$

With Q_{exch} the exchange flow between the river and the aquifer which is negative when water flows from the river to the aquifer, H_{gw} the piezometric head in the aquifer, H_{riv} the water head in the river, and Q_{dis} the available flow in the river cell. Q_{lim} is a maximum infiltration flow

from the river to the aquifer, corresponding to the case when the aquifer head is below the river bed (Rushton, 2007). A steady river head H_{riv} is usually considered in MODCOU, however, due to the impact of river-aquifer interactions in the Rhine hydrosystem, time varying heads based on observations were included for the Rhine River, as well as for the Hardt Canal. This waterway is used for irrigation purposes, and preliminary results have shown it was important to explicitly simulate its losses to the aquifer.

MODCOU uses a daily time step to allow a better estimation of the river-aquifer exchange dynamics.

MODCOU can also be coupled with the soil-vegetation-atmosphere transfer scheme ISBA (Noilhan and Planton 1989) to form the SIM model (Habets et al., 2008). SIM is used here to have another estimation of the effective rainfall infiltration over the aquifer.

3.2 HPP-INV

The HPP-INV model (Chardigny 1999, Majdalani and Ackerer, 2010) is a modelling tool using an inversion algorithm in order to assess aquifer hydrodynamic parameters. It is based on a classical hydrogeological model, and includes an adaptative multiscale triangulation for the inversion algorithm (Majdalani and Ackerer, 2010).

Piezometric levels simulation is based on a finite elements scheme and the river flows are simulated with a Muskingum scheme (Majdalani and Ackerer, 2010). Rivers-aquifer interactions are computed from the difference between river and aquifer heads, with transfer coefficients values calibrated during the inversion process (LUBW, 2006). In the present application, this model is run at a monthly time step.

There is no computation of a surface water budget, and groundwater recharge by rainfall is provided by MODCOU. Moreover, the model is limited to the aquifer in the plain, and the lateral inflows from bordering catchments are calibrated.

The inversion method used to derive the spatial distribution of permeability is based on minimization of the error between simulated and observed piezometric heads and river flow data. Several distributions can be obtained according to different inversion conditions.

4. Model set up

4.1 Discretization

The area modelled with MODCOU corresponds to the Rhine basin between Basel in the South and Lauterbourg in the North. The basin total area is approximately 13900 km², and the area of the alluvial aquifer is 4655 km² (Figure 3). Two different boundary conditions are imposed: the Rhine river discharge at Basel, and fixed piezometric heads at the northern and southern boundaries.

The basin was discretized with square cells ranging in size from 200 m for the river cells to 1600 m. There are 99715 surface cells, and 34180 aquifer cells (Figure 3). The alluvial aquifer is represented with a single layer.

Subsurface flow at the western and eastern borders of the aquifer is known to be a significant part of the recharge (LfU, 1996, LUBW, 2006). It is represented by specific boundary conditions in the model: the surface runoff reaching the aquifer surface on the bordering cells infiltrates to the water table and thus contributes to the aquifer recharge. This process is called hereafter lateral subsurface flow.

Figure 3 : a) Discretization of the surface (light red) and the aquifer parts (green) of the model. The border cells where the surface runoff is infiltrating are plotted in dark brown ; b) Land use data extracted from Corine Land Cover 2000 data set.

Uncertainty on the components of the water budget is evaluated by exploring several equally probable hydrodynamic parameter sets (permeability, transfer coefficient, maximum river infiltration flows) as well as two estimations of the water budget from the SIM land surface scheme, and the MODCOU production functions. Consequently, only the best parameter set for the production functions, obtained through calibration, was considered to run MODCOU. The calibration method is presented in the following section.

4.2 Calibration of the surface water budget model

The parameter calibration process can be problematic, because of non-uniqueness (see for example Beven, 1993; Gupta et al, 1998; Refsgaard, 1997). To avoid this kind of issues during the calibration process, the number of parameters to be adjusted is usually reduced. A manner to do this is to assess values for parameters based on their physical significance in the hydrosystem. However the spatial distribution of these physical parameters is often not well known, and the point measurement values may not be representative of grid cell scale parameters. Moreover, model parameters are not always easily linked to physical properties of the system. This is the case for the production function parameters of the MODCOU surface model (Figure 4), which allow partitioning the incoming rainfall between actual evapotranspiration and effective rainfall, and of effective rainfall between infiltration and surface run-off. The values of the parameters are not connected to observed variables and are most often calibrated.

Figure 4 : schematization of a production function in MODCOU for surface water budget computation
(Ledoux et al., 1989)

Calibration of the water budget is based on the reduction of errors between observed and simulated rivers flows. River gauges out of the Rhine alluvial plain were used to calibrate the production functions, considering that the contribution of aquifer-rivers interactions at these gauging stations is negligible.

This calibration was carried out in a two steps process, with first calibration of the water volumes flowing at the gauging stations, and then of river flow dynamics.

Ten gauging stations in the Vosges Mountains and in the Sundgau area were selected, based on the repartition of the main production functions on their drainage areas. Twenty one production functions were defined on this area, crossing information on land use (Corine Land Cover) and geological soil types (from geological maps). The parameters were calibrated for the fourteen production functions representing more than 20 km² on the gauging stations watersheds, as the influence of the other production functions was not sufficient over these areas. The parameters from the ten remaining production functions were set according to similar soil and vegetation types in previous applications (Golaz et al.2001, Gomez et al, 2003, Korkmaz et al., 2009).

Calibration was performed in a semi automatic way, by testing several predefined values for each parameter. The calibration period was from August 2000 to December 2003, as this period presents contrasted climatic conditions, and has almost complete daily river flow measurements for the selected gauging stations.

For each of the fourteen production functions, five reservoir parameters were adjusted. First the parameters determining the total volume of water flowing at a gauging station (CRT and DCRT) were calibrated based on the relative difference between simulated and observed water volumes over the calibration period following equation 2.

$$\sum_{i=1}^{n_{stations}} \left| \frac{V_{obs,i} - V_{sim,i}}{V_{obs,i}} \right| \times \frac{1}{n_{stations}}, \quad (2)$$

$n_{stations}$ being the number of gauging stations used for calibration, $V_{sim, i}$ the simulated, and $V_{obs, i}$ the observed volumes of water flowing at a station i .

Then the parameters affecting only the dynamics of river flow (FN, CQI and CQR) were calibrated by optimizing the Nash efficiency (see § 5.1).

Only the best set of parameters was kept, as the sensitivity of the model to groundwater recharge is assessed by using the water budget from the SIM model, as explained below.

5. Assessment of the hydrogeological simulations

In order to address the uncertainty in the aquifer water budgets and specifically recharge components, several simulations using different equiprobable parameter sets were performed. Some well constrained parameters were fixed (e.g. calibrated production functions parameters, specific storage), while unconstrained hydrodynamic parameters that influence 1/ the transfer dynamic, 2/ the computation of rivers-aquifer interactions, and 3/ the aquifer recharge were investigated.

1/ Transmissivity: Several distributions were obtained with HPP INV, by using various initial conditions or criteria. These distributions are in good agreement with experimental data from pumping tests (Majdalani and Ackerer, 2010). Four contrasted distributions were tested in the present study to assess the sensitivity of the model to this parameter (Figure 5 and Table 1). Two sets have similar mean values, but contrasted standard deviations, and the two others have higher and lower mean values.

2/ To investigate the uncertainty on the river aquifer interactions, the sensitivity of the model to three parameters was tested:

a) The maximum river infiltration rate to the aquifer, for river cells of 200 m: $Q_{lim} = 0$ (i.e. no infiltration), 25, 50 and 100 L/s (see Equation 1). This parameter influences surface /

groundwater interactions, exclusively in the direction of river infiltration towards the water table.

b) The transfer coefficients between the surface and the groundwater parts of the model: the initial value of 0.05 m²/s was multiplied by 2 and by 10. This parameter has an influence over the surface-aquifer interactions in both directions.

c) The Rhine River and the Hardt canal heads: the impact of the variation with time of these river heads on the aquifer and streamflows behaviours was assessed. Although the Hardt canal has far smaller discharges than the Rhine River, preliminary results and KLT analysis have shown that it was important to represent this irrigation waterway. For this canal it was also tested not taking into account variable water flows.

3/ Uncertainty in the surface water balance is taken into account by using two estimates of the infiltration rates: one from MODCOU (conceptual model), and the other from SIM (ISBA land surface scheme). The latter leads to an infiltration reduced by about 23 %.

Figure 5 : Two of the four transmissivity distributions tested, obtained through inversion with the HPP INV model.

The specific storage distribution used is the same as in Majdalani and Ackerer (2010), with values of 0.05 everywhere, except along a band a few kilometres wide around the southern part of the Rhine River, where the value is 0.12.

A reference simulation, based on mean range parameters (Table 1), is considered in order to assess the impact of different parameters variation independently: eleven other simulations were run by modifying a single parameter values at a time. Table 1 summarizes the different parameters values tested.

Simulation	Transmissivities (mean value and standard deviation in m ² /s)	Maximum infiltration flow Q_{lim}	Transfer coefficient T_p	Infiltration rate Q_i
Reference	Hpp19 (0.415; 0.426)	50 L/s	0.05 m ² /s	MODCOU
T hpp18	Hpp18 (0.415; 0.457)	50 L/s	0.05 m ² /s	MODCOU
T hpp47	Hpp47 (0.438; 0.465)	50 L/s	0.05 m ² /s	MODCOU
T hpp103	Hpp103 (0.377; 0.412)	50 L/s	0.05 m ² /s	MODCOU
$Q_{lim} = 0$	Hpp19	0 L/s	0.05 m ² /s	MODCOU
$Q_{lim} = 100$ L/s	Hpp19	100 L/s	0.05 m ² /s	MODCOU
$Q_{lim} = 25$ L/s	Hpp19	25 L/s	0.05 m ² /s	MODCOU
$T_p = 0.1$ m ² /s	Hpp19	50 L/s	0.1 m ² /s	MODCOU
$T_p = 0.5$ m ² /s	Hpp19	50 L/s	0.5 m ² /s	MODCOU
SIM	Hpp19	50 L/s	0.05 m ² /s	SIM
Steady H Rhine	Hpp19	50 L/s	0.05 m ² /s	MODCOU
Steady H & Q Hardt	Hpp19	50 L/s	0.05 m ² /s	MODCOU

Table 1 : Recapitulation of the different model parameterizations tested

5.1 Standard analysis

Results obtained with the different parameterizations are quantitatively evaluated in terms of river flows using Nash criterion, and of piezometric levels using biases.

5.1.1. Comparison of the riverflows

Nash criterion (Nash and Sutcliffe, 1970) is a measure of fit between observed and computed values (Equation 3). Its optimal and maximal value is 1 and its minimum value is $-\infty$. A zero value indicates that the model does not perform better than the mean value of the observations.

$$Nash = 1 - \frac{\sum_{i=1}^n (Q_{obs,i} - Q_{sim,i})^2}{\sum_{i=1}^n (Q_{obs,i} - \bar{Q}_{obs})^2}, \quad (3)$$

with n the number of observed values, $Q_{obs,i}$ the observed river flows, $Q_{sim,i}$ the simulated river flows, with i denoting the time step, and \bar{Q}_{obs} the arithmetic mean of the observed river flows.

The distribution of Nash criteria for the twelve simulations is shown at each gauging station (Figure 6). General agreement between simulated and observed river flows is found on most mountainous catchments, although some stations have low criterion values. Main discrepancies are located in the plain, which can be explained by the difficulty to reproduce the complex interactions between rivers and the aquifer in this area, and also by an important regulation of discharges in some rivers. The poor results on the German side can be linked to the poorer reconstitution of the atmospheric forcing, as less local climatic data were used in the SAFRAN analysis in Germany. There is no variation between the different simulations in the mountainous catchments as the different parameters tested have no influence on these catchments. The criterion presents some variability in the plain, especially on the Ill River.

Figure 6 : Spatial distribution of the daily Nash criterion values. At each gauging station a pie is plotted representing the distribution of the Nash criterion values for the 12 simulations.

However, the parameters have a more pronounced impact on low flows. Indeed, the 5-year return period low flow (QMNA5) can almost double from a simulation to another, especially in the southern part of the plain (not shown).

5.1.2. Piezometric levels comparison

Piezometric levels biases are computed as the average difference between simulated and observed piezometric heads.

$$Bias = \frac{1}{n} \sum_{i=1}^n (H_{sim,i} - H_{obs,i}), \quad (4)$$

Here n is the number of observed values, $H_{sim,i}$ the simulated piezometric levels, $H_{obs,i}$ the observed piezometric levels, i denoting the time step.

Figure 7 : Comparison between observed and simulated piezometric levels at the 190 observation wells over the 1986-2002 period. Left: bias [m] computed for the reference simulation, middle: mean bias [m] for the 12 simulations, right: standard deviation of the bias over the 12 simulations [m].

Figure 7 shows the spatial distribution of the piezometric levels biases for the reference simulation as well as the mean bias and its standard deviation for the 12 simulations in meter. The piezometric levels are underestimated in the South Western part and rather well estimated in the centre of the plain. The sensitivity of the parameters tested is higher in the Southern part of the aquifer, with large standard deviations. Indeed in this area piezometric levels are strongly influenced by river infiltration. Some simulations better represent the observed piezometric levels in the South, as illustrated with the reference simulation results.

Figure 8 : Bias histogram computed on the 190 observation wells, for the twelve simulations

Figure 8 shows the statistical distributions of the 190 biases computed for each of the twelve simulations. The distributions show that most observations are well reproduced by the models, the largest number of observation wells being associated with the lowest errors. Only the simulation with no infiltration of rivers to the aquifer ($Q_{lim}=0$) shows a distinct pattern, with more negative biases. This underlines the importance of the river to aquifer flux.

Compared to the reference simulation, a maximum infiltration rate set to $Q_{lim}=100$ L/s leads to an overestimation of the piezometric levels, with more observation wells having bias values ranging from 1 to 5 m, while the reduced value of this maximum infiltration rate ($Q_{lim}=25$ L/s) leads to slightly less values close to 0. The modification of the transfer coefficient for surface/groundwater exchange (T_p) leads to a greater number of negative biases values, but mainly in the range between -2.5 and -1 m.

It is rather difficult to distinguish the results obtained by the four transmissivity distributions, and by the two infiltration rates.

Not taking into account the variations of the Rhine water levels leads to more overestimated piezometric levels, whereas steady values for the Hardt Canal water levels and flow lead to more underestimated levels.

Similar results were obtained for the root mean square error (not shown) for which the maximum dispersion is reached for the $Q_{lim} = 0$ simulation.

From these comparisons, it is clear that classic statistical results are not sufficient to discriminate the various sets of parameter and that all the simulations except the one with no river infiltration give rather comparable results. In order to go further in the analysis of the simulations, we used a more advanced tool, the Karhunen Loève Transform.

5.2 Analysis using the Karhunen-Loève transform method

5.2.1 Principle of the piezometric data analysis

Longuevergne et al. (2007) have performed a statistical analysis (Karhunen-Loève transform, hereafter KLT) to separate the main influent processes on piezometric variability from observed time series. KLT, similar to Principal Components Analysis (Wilks, 1995), involves summing up a set of possibly correlated time series into a few uncorrelated variables called eigenvectors Y_k , related to the original variables by an orthogonal transformation maximizing

explained variance. Piezometric head time series, expressed as the variation around the mean level, may then be simply reconstructed as a sum of the temporal behaviours (eigenvectors

$$Y_k(t)) \text{ with associated spatial weight } a_k^{obs}: \Delta H_{obs}(t) = \sum_k a_k^{obs} Y_k(t)$$

This method was already applied on the Upper Rhine aquifer piezometric observations (Longuevergne et al., 2007). Several eigenvectors describing the global temporal behaviour of the aquifer were extracted and interpreted as different contributions to groundwater variations, namely mountain rivers interactions, effective rainfall and Rhine river interactions for the three more important ones. The analysis of the weights a_k^{obs} at 190 observation wells allows describing the spatial distribution of these different influences. The results showed that nearly 70% of the aquifer behaviour is determined by interactions with rivers, with a distinction between the Rhine River and the other ones.

In the present study, the Karhunen Loève method is also applied to each simulation in order to assess how well it reproduces the processes involved in the observed piezometric time series. For this purpose, the model results were projected on the eigenvectors Y_k obtained from observations to compute spatial information a_k^{sim} for each model and compare them with spatial information from observations, for each separate process described by the eigenvectors, allowing a multi-criterion analysis of the model quality.

5.2.2. Decomposition of the simulated piezometric time series

The five main eigenvectors Y_k (interpreted as specific processes) determined by KLT of the piezometric data were able to explain more than 80% of the aquifer behaviour (Longuevergne et al., 2007).

477 The associated weights a_k^{obs} for each well are compared to those obtained by projection of the
 478 model results on the eigenvectors Y_k , a_k^{sim} , for each simulation. As eigenvectors are
 479 orthogonal, the root mean square error (RMSE) between model and observations may be
 480 simply written as $\|H_{obs}(t) - H_{sim}(t)\|^2 = \sum_{k=1}^5 (a_k^{obs} - a_k^{sim})^2 \|Y_k(t)\|^2 + \varepsilon$, where ε is a truncation
 481 error (only the five first eigenvectors are considered here). Minimization of the root mean
 482 square error may be carried out on the spatial information, for each eigenvector associated
 483 with highlighted processes.

484 The first eigenvector (Figure 9), related to the contribution of mountain rivers, explains nearly
 485 50% of the aquifer behaviour. Specifically, variations in annual river discharge at the entrance
 486 of the plain where the aquifer lies are closely related to long-term signature of the first
 487 eigenvector (Figure 9 a). Spatially, the contribution of the first eigenvector to observations is
 488 more important on the mountain piedmont than along the Rhine River (Figure 9 b). The same
 489 map can be drawn for the reference simulation, considering the same eigenvector (Figure 9 c),
 490 and the difference between the two maps highlights the model error (Figure 9 d). Globally, the
 491 agreement is quite good and differences are localized in specific areas. For example, the
 492 impact of mountainous rivers seems to be underestimated on the mountain piedmont north of
 493 Colmar only. On contrary, the impact is overestimated along the Rhine River and in the areas
 494 which are known to be highly anthropized (canals north of Basel, Mulhouse area affected by
 495 potash mines and artificial lakes south of Strasbourg).

496 The method allows pointing out areas where the contribution of each process to the head
 497 variability is not properly reproduced by the model. This spatial information may also be
 498 interpreted globally as statistical information to assess the ability of the different simulations
 499 to capture the global behaviour of the aquifer system (Figure 10). Ideally, the distribution of

$a_k^{sim} - a_k^{obs}$ for the 190 observation wells and for a given simulation should be centred on zero with reduced dispersion, for each eigenvector.

For example, considering no river infiltration drives to significant underestimation of the impact of the first eigenvector, corresponding to the contribution of mountainous rivers. Figure 10 shows that the maximum river infiltration flow of 100 L/s, gives larger errors, and thus, that this parameter set is less probable than others.

The largest contribution to RMSE for all simulations is concentrated on the second eigenvector (Figure 10) previously interpreted as the contribution of effective rainfall. The examination of spatial errors highlights strong differences in the Southern and Eastern parts of the domain. However, the error is reduced when taking into account even partially impact of irrigation in the Hardt area (Noyer and Elsass, 2006), since the error is larger for the simulation without varying water flows and levels in the Hardt irrigation canal (Figure 10)

Analysis of the differences on the third eigenvector, related to the impact of the Rhine River, clearly indicates that both infiltration and Rhine river level variations are important processes to describe the interactions between the Rhine River and the aquifer. It also underlines that varying the transfer coefficient values (T_P) can be interesting for a better representation of the Rhine river influence over the aquifer.

Figure 9: Spatial and temporal analysis with the KLT method for the first eigenvector, associated with the influence of mountain rivers over groundwater variability. a) First eigenvector time series; b) and c) Maps of the weights associated with the first eigenvector for the observations and reference simulation respectively; d) Map of the differences between simulated and observed weights.

Figure 10: Errors in the reproduction of the eigenvectors weights at the 190 observation wells for the twelve simulations a) Mean total errors for the five eigenvectors and standard deviations ; b) Contribution to the total error of eigenvectors 1, 2 and 3.

527

528 The four transmissivity distributions tested perform equally well to describe the impact of the
529 mountainous rivers. Hpp103 shows slightly larger underestimation North of Colmar, but also
530 smaller overestimation in Strasbourg area. In the meantime this distribution, which has the
531 lowest mean value, generates less error on the third eigenvector, which has more energy along
532 the Rhine River, and more error on the second eigenvector, representing the rainfall influence.
533 The statistical analysis of the simulations has shown that one of the twelve simulations,
534 “ $Q_{lim}=0$ ”, failed to reproduce the behaviour of the basin, and that two others, “Steady H&Q
535 Hardt” and “ $Q_{lim} = 100 \text{ L/s}$ ”, are less probable although they cannot be completely rejected.
536 The nine remaining simulations cannot really be distinguished statistically, and, although
537 there are still some errors in the representation of the hydrosystem, these nine simulations
538 represent equally well the basin functioning.

539

540 **6. Analysis of the water fluxes**

541 **6.1 Surface-aquifer exchange flux**

542 Surface-aquifer exchange is known to be one key component of the aquifer water budget,
543 although only few quantified estimations based on observations are available.
544 Figure 11 shows the average and the standard deviation of the simulated mean exchange
545 flows on the period for the nine acceptable simulations. This map highlights the main
546 drainage and river infiltration zones of the hydrosystem. Simulated river infiltration flows
547 (blue cells on Figure 11) are high in the Southern part of the aquifer, mainly along the Rhine
548 River. They are also important in Strasbourg area. These correspond to zones where the
549 infiltration of rivers is known to be important, especially in the Southern part of the plain
550 where several studies have given quantitative estimations of the recharge from the rivers to
551 the aquifer (Esteves, 1989, George et al., 1995).

In most part of the domain, the surface-aquifer exchange present low variability (standard deviation values close to 0) except in some parts near the centre of the aquifer (Figure 11).

Figure 11: Mean exchange fluxes between the surface and the aquifer for the reference simulation (left) and on average on the 9 simulations (centre), and its relative standard deviation (right)

Water table drainage zones (green to red cells on the left and middle maps of Figure 11) occur in the Southern part of the aquifer, near its borders and along the Rhine River. Drainage zones extensions are quite important in the centre of the plain between Colmar in the South and Strasbourg in the North. This corresponds to the Ried area, an important wetland with shallow water table, leading to an important aquifer overflow and the presence of groundwater-fed streams.

In the Northern part of the aquifer, important drainage flows from the aquifer occur, due to the proximity of the water table to the topographic surface.

Comparisons were made with values found in the literature (PIREN Eau Alsace, 1984; Esteves, 1989; George et al., 1995; Schmitt, 2001). These values often correspond to limited space and time extents, but it is interesting to know whether the orders of magnitude of the simulated exchange are plausible.

Esteves (1989) indicates an average infiltration flow of 200 to 300 L/s on the Fecht River between its entry into the plain and its confluence with the Weiss River. On this reach an infiltration flow of 1000 L/s is simulated on average. Downstream the drainage flow varied from 100 to 300 L/s on average (Esteves, 1989), whereas MODCOU results give an average of 1635 L/s. Thus for this river the intensity of the exchange is certainly overestimated by the model.

Along the Ill River, Esteves (1989) gives a value of 200 L/s/km infiltrating from the river to the aquifer between Ensisheim and Colmar. The PIREN Eau Alsace (1984) gives a value of 130 L/s/km infiltrating between Ensisheim and Oberhergheim, and 37 L/s/km between Oberhergheim and Horbourg-Wihr, for the period 1971-1974. George et al. (1995) estimate the infiltration between Mulhouse and Ensisheim amounts to 65 L/s/km in average.

The simulated exchange flows give an average infiltration of 124 L/s/km between Mulhouse and Ensisheim, 93 L/s/km between Ensisheim and Oberhergheim, 87 L/s/km between Oberhergheim and Horbourg-Wihr and 79 L/s/km between Ensisheim and Colmar.

Thus simulated infiltration of the Ill River between Mulhouse and Colmar is less variable than estimated by observations, and it is overestimated upstream of Ensisheim and downstream of Oberhergheim, while it seems underestimated between Ensisheim and Oberhergheim, i.e. on the section just downstream of the confluence with the Thur River. However most of these estimates are made by punctual gauging, a method lacking precision, and giving results with time limited representativeness. Similar results are found on the Thur and Doller rivers, at the South western end of the basin (George et al. 1995, Schmitt 2001).

It comes to the conclusion that the MODCOU model with the selected parameter sets is able to represent the main spatial pattern of the aquifer-surface interactions. However, it has some difficulties capturing the spatial variability of the exchange even by using several parameter sets. On average this flux is overestimated in some sections of the hydrographic network. This is probably due to the use of spatially homogeneous distribution for the parameters T_p and Q_{lim} directly influencing the river-aquifer exchange.

6.2 Water Budgets

In order to address uncertainties in the functioning of the Upper Rhine aquifer, an analysis of the water budgets computed by the different simulations is performed.

Figure 12: Mean annual partition of the aquifer inflows between lateral subsurface flow, effective rainfall and river infiltration (right bars), and of the aquifer outflows between pumping and rivers drainage (left bars).

Figure 12 shows the water budget for the aquifer recharge and discharge for the nine plausible simulations. All the simulations, except the one with the effective rainfall infiltration scaled according to SIM have the same effective rainfall and lateral subsurface flow recharge rates. The river infiltration rate is the most important and most variable flux between the different simulations. This flux almost doubles from the simulation $Q_{lim} = 25$ L/s to the simulation $T_p = 0.5$ m²/s. For the nine simulations, it represents about 80 % of the aquifer recharge, with a maximum of 82 % for the simulations $T_p = 0.5$ m²/s and $Q_i \cdot 0.77036$ and a minimum of 74 % for the simulation $Q_{lim} = 25$ L/s. The nine simulations allow estimating the river infiltration flux to 115 ± 16.5 m³/s, thus with an uncertainty of 14 %. Considering the twelve simulations, the flux estimates would have been more scattered, with an average value of 105 ± 37 m³/s. Therefore, the KLT analysis allowed reducing the uncertainty from 35% to 14%. These results are consistent with those obtained in the framework of the LIFE project. A value of 85 % was found with a steady state simulation for a low water situation (LfU, 1996). On the contrary in the Monit project the main contribution to the recharge of the aquifer was found to be the effective rainfall infiltration over its surface (LUBW, 2006). The lateral subsurface flow is about two times lower than the effective rainfall infiltration, and represents approximately 7% of the water budget. The main output process in all cases is the drainage of the aquifer by the rivers and by overflow. Another interesting variable is the aquifer storage variations. To analyse the uncertainty on this variable according to the parameter sets, the evolution of the aquifer storage were converted into water height variations over the entire surface of the aquifer. Thus, a variation

of 1 mm over the whole aquifer represents an evolution of the aquifer volume of 4,655,000 m³.

These variations are computed by reference to the aquifer stock at a given date, namely the 30th July 1986. This date was chosen in order not to take into account variations during the first year of simulations, which could be due to inaccurate estimates of initial piezometric levels.

Figure 13: Monthly aquifer stock evolution from 1986 to 2003 as estimated by the 9 acceptable simulations

The nine simulations present similar evolution of the aquifer stock. The largest discrepancy is associated to the simulation with reduced maximum river infiltration rate. For the outlier simulation without river infiltration ($Q_{lim} = 0$ L/s) the stock decreases by about 500 mm (not shown). When the maximum river infiltration rate is set to $Q_{lim} = 25$ L/s, the aquifer stock is reduced by approximately 25 mm at most.

The stock variations are not very sensitive to the transmissivity distributions although the differences between the four distributions can reach 10 mm at some periods (Figure 13).

The different transfer coefficient values (T_p) lead to quite similar stock variations, even for the higher value of $T_p = 0.5$ m²/s, which was shown to be the case having the highest river infiltration flow. In this case, the stock is increased by only a few millimetres. Indeed there is compensation between the river infiltration and drainage rates leading to a similar evolution of the aquifer storage.

The reduced rainfall infiltration computed by SIM also has a limited impact on the aquifer storage variations. Indeed the maximum impact reaches 10 mm at most between the reference simulation and the reduced infiltration simulation.

To summarize, the aquifer stock variations are rather sensitive to the maximum river infiltration rate, whereas they are less sensitive to rainfall infiltration and to transfer coefficients. This can be explained by the fact that a modification of the infiltration over the aquifer surface is balanced by a modification of the exchange with rivers flowing from the mountains. Increasing the transfer coefficients leads to larger exchange between the aquifer and the surface in both directions. This phenomenon can explain why the aquifer stock is not really affected. On the other hand when the maximum river infiltration rate is modified, it only affects the exchange from the rivers to the aquifer, leading to increased aquifer stock variations.

Conclusion

The objective of the study was to increase understanding of the Upper Rhine Graben aquifer functioning. Modelling of the Upper Rhine graben aquifer was performed with the MODCOU coupled hydrogeological model computing the surface water budget, groundwater flow and interactions between the aquifer and the surface. Distributions of aquifer transmissivities were provided by the inversion algorithm of the HPP-INV hydrogeological model. In the present study, the sensitivity of the MODCOU model results to some model parameters governing the surface / groundwater interactions was assessed, specifically in terms of aquifer behaviour. Although the developed model is not suited to represent fine scale processes and fully coupled interactions between surface water and groundwater, it represents the main processes that impact the aquifer water budget, and thus, allows an analysis of their spatial distribution.

Twelve model runs were performed using several parameter sets for the transmissivity, the surface/groundwater transfer coefficient, the maximum river infiltration flow, Hardt Canal

water levels and flows and Rhine river water levels, and two estimations of the surface water budget in the plain.

These twelve runs were assessed using classic statistical criteria: the daily Nash efficiency for the river flows, and biases for the piezometric levels. These analyses show that for each run, the model had some problems reproducing the daily discharges on the German side, probably due to some weaknesses of the atmospheric analysis using fewer meteorological stations in Germany than in France. The biases on the simulated piezometric heads are rather weak except on the southern part of the basin, where the discrepancy between the twelve simulations is large. These classical analyses were able to highlight that one set of parameters was not coherent with the functioning of the aquifer system, and thus that it is required to take into account the possibility for rivers to infiltrate.

In order to go further in the assessment of the simulations results, a mathematical analysis method based on a Karhunen Loève transform (KLT) of piezometric time series was used to analyse the simulated piezometric levels temporal variations, as well as the observed ones. This method allows separating the different processes influencing the water table evolution, in the form of eigenvectors representing river infiltration and the effective rainfall influences. The spatial distribution of the projections stemming from the decomposition of piezometric chronicles as linear combinations of the eigenvectors allows having an idea of the area of dominating influence of the three main processes. Comparison of the projections obtained with simulated and observed piezometric time series also highlights the main areas where difficulties arise to reproduce the water table behaviour. KLT showed that all model runs failed to represent the annual component of the second eigenvector, related to the impact of effective rainfall, mainly due to large errors in the Hardt area in the south of the domain, and in the Eastern part of the plain. This error is however reduced when taking into account the irrigation practises in the Hardt area, with irrigation water flowing through channels with high

bed permeability and thus large river-aquifer exchanges. The KLT method underlines the need to better take into account these processes in the model. This method also proved an interesting and original technique to assess the model performances in reproducing the spatial and temporal variability of water table levels, as well as the recharge/discharge processes inducing these variations. It might be considered using this method in order to test spatial patterns of some parameters taken homogeneous for now, such as the transfer coefficient T_p and the maximum river infiltration rate Q_{lim} .

Comparison of the aquifer water budgets obtained with different parameter sets shows that there is a balance between the magnitude of river to aquifer infiltration and drainage of the aquifer so that the aquifer stock is rather stable for each run.

The intensity of the simulated river-aquifer exchange was compared to available observations, mainly on the Ill River. Estimated values are in the same order as the observed ones. However the model presents smoother spatial variations of the simulated fluxes than observed, which could be due to the use of spatially homogeneous river bed parameters.

The KLT method has shown that nine over twelve simulations were able to have a similarly satisfying representation of the aquifer behaviour. This allows reducing the uncertainty of aquifer recharge by river infiltration from 35 % to 14 % with an average flux of 115 m³/s. This represents about 80% of the aquifer inflow.

This proportion compares well to the LIFE project estimate for a low water situation, but is more important than the one from the Monit project for a transient state simulation.

This study brings increased comprehension of the functioning of an alluvial aquifer, which is strongly influenced by groundwater /surface water interactions. It shows that modelling, together with inversion and advanced statistical methods are powerful tools to quantify the water budget of an alluvial aquifer.

Future work will include a climate change impact study on this vulnerable aquifer, by taking into account the uncertainty associated with emission scenarios, climate models, and hydrogeological model parameters.

Acknowledgements

This work was supported by the program VMC-2007 of the French Agence Nationale de la Recherche (ANR) under the project VULNAR.

We would like to thank the different persons and institutions who provided us with data for the modelling, especially: Michel Wingerling at the LUBW for German hydrometric data; Dr. Werner Weinzierl and Dr Frank Waldmann at the LGRB for the German soil type data; Philippe Elsass at the BRGM for its help in the understanding of the Upper Rhine hydrosystem; Jean Lett and Claude Husser at the Navigation Service of Strasbourg for the Rhine River levels data; Joëlle Sauter at the ARAA for the French soil data.

References

- Allen D M, Mackie D C, Wei M (2004) Groundwater and climate change: a sensitivity analysis for the Grand Forks aquifer, southern British Columbia, Canada. *Hydrogeology Journal*, **12**, 270-290.
- Bauer M, Eichinger L, Elsass P, Kloppmann W, Wirsing G (2005) Isotopic and hydrochemical studies of groundwater flow and salinity in the Southern Upper Rhine Graben. *International Journal in Earth Sciences*, **94**, 565–579.
- Beven K (1993) Prophecy, reality and uncertainty in distributed hydrological modelling. *Advances in Water Resources*, **16**, 41–51.
- Beven K. (2006) A manifesto for the equifinality thesis. *Journal of Hydrology*, **320**, 18-36.
- Camporese, M., Paniconi, C., Putti, M., & Orlandini, S. 2010. Surface-subsurface flow modeling with path-based runoff routing, boundary condition-based coupling, and assimilation of multisource observation data. *Water Resources Research*, **46**.
- Chardigny E (1999) *Modelisation de l'hydrodynamique des eaux souterraines (Modelling the groundwater hydrodynamics)*. Ph.D. thesis, Universite Louis Pasteur, Strasbourg.
- David C, Habets F, Maidment D R, Yang E L (2011) Rapid applied to the SIM-France model. *Hydrological Processes*, doi: 10.1002/hyp.8070
- Duprat A, Simler L, Valentin J (1979) *Sciences Geologiques - La nappe phreatique de la plaine du Rhin en Alsace (The phreatic water table of the Rhine Plain in Alsace)*. CNRS.
- Esteves M (1989) *Etude et modelisation des relations aquifere-riviere dans le Ried de Colmar (Haut-Rhin, France) (Study and modelling of the aquifer-rivers relations in the Colmar Ried)*. Ph.D. thesis, Universite Louis Pasteur, Strasbourg.

763 George M, Calmbach L, Lettermann M, Menillet F, Baderot S (1995) *Carte hydrogéologique*
764 *Suisse a 1/100000 - Feuille Basel/Bale (The hydrogeologic map of Switzerland - Basel*
765 *leaf)*. Tech. rept. BRGM.

766 Golaz-Cavazzi C, Etchevers P, Habets F, Ledoux E, Noilhan J (2001) Comparison of two
767 hydrological simulations of the Rhone basin. *Physics and Chemistry of the Earth*, **26**,
768 461–466.

769 Gomez E., Ledoux E., Viennot P., Mignolet C., Benoit M., Bornerand C., Schott C., Mary B.
770 Billen G., Ducharne A., Brunstein D. (2003) Un outil de modélisation intégrée du
771 transfert des nitrates sur un système hydrologique : application au bassin de la Seine
772 (An Integrated Modelling Tool for Nitrates Transport in a Hydrological System:
773 Application to the River Seine Basin), *La Houille Blanche*, **3**, 38-45

774 Gupta H. V., Sorooshian S., Yapo P. O. (1998) Toward improved calibration of hydrologic
775 models : Multiple and noncommensurable measures of information. *Water Resources*
776 *Research*, **34**, 751–763.

777 Habets F., Boone A., Champeaux J. L., Etchevers P., Franchistéguy L., Leblois E., Ledoux E.,
778 Le Moigne P., Martin E., Morel S., Noilhan J., Quintana Seguí P., Rousset-Regimbeau
779 F., Viennot P. (2008) The SAFRAN-ISBA-MODCOU hydrometeorological model
780 applied over France, *Journal of Geophysical Research*, **113**

781 Hu L T, Chen C X, Jiao J J, Wang Z J (2007) Simulated groundwater interaction with rivers
782 and springs in the Heihe river basin. *Hydrological Processes*, **21**, 2794–2806.

783 Illies J H (1972) The Rhine graben rift system-plate tectonics and transform faulting. *Surveys*
784 *in Geophysics*, **1**, 27–60.

785 Kalbus E, Reinstorf F, Schirmer M (2006) Measuring methods for groundwater–surface water
786 interactions: a review. *Hydrology and Earth System Sciences*, **10**, 873–887

787 Kollet S J, Maxwell R M (2006) Integrated surface–groundwater flow modeling: A free-
788 surface overland flow boundary condition in a parallel ground water flow model.
789 *Advances in water resources*, **29**, 945–958.

790 Konikow L. F., Bredehoeft J. D. (1992) Ground-water models cannot be validated. *Advances*
791 *in water resources*, **15**, 75–83.

792 Korkmaz S. (2007) *Modeling of the flood regimes in coupled stream-aquifer systems*, Phd
793 Thesis, Ecole des Mines, Paris and Middle East Technical University, Ankara.

794 Korkmaz S, Ledoux E, Onder H (2009) Application of the coupled model to the Somme river
795 basin. *Journal of Hydrology*, **366**, 21–34.

796 Ledoux E., Girard G., de Marsily G., Deschenes J. (1989) Spatially distributed modeling:
797 conceptual approach, coupling surface water and groundwater. In : *Unsaturated Flow*
798 *Hydrologic Modeling-theory and Practice - Arles, France, 13-17 June 1988*

799 Ledoux E, Gomez E, Monget J M, Viavattene C, Viennot P, Ducharne A, Benoit M, Mignolet
800 C, Schott C, Mary B (2007) Agriculture and groundwater nitrate contamination in the
801 Seine basin. The STICS-MODCOU modelling chain. *Science of the Total*
802 *Environment*, **375**, 33–47.

803 LfU (1996) *Action de démonstration portant sur la protection et la gestion des réserves en*
804 *eau souterraine dans la partie franco-germano-suisse de la vallée du Rhin Supérieur –*
805 *Rapport final (Demonstration action on protection and management of groundwater*
806 *resources in the french-german-swiss part of the Upper Rhine valley – Final report).*
807 Tech. rept. Landesanstalt für Umweltschutz Baden-Württemberg.

808 LfU. (2005) *MONIT: Développement des outils de prévision (MONIT : developement of*
809 *prevision tools).* Tech. rept. Landesanstalt für Umweltschutz Baden-Württemberg.

810 Longuevergne L, Florsch N, Elsass P (2007) Extracting coherent regional information from
811 local measurements with Karhunen-Loève transform : case study of an alluvial aquifer
812 (Rhine Valley, France and Germany). *Water Resources Research*, **43**, 13.

813 LUBW (2006) *Projet INTERREG III Monit : Modelisation hydrodynamique et transport des*
814 *nitrates (INTERREG III project Monit : Hydrodynamic modelling and nitrates*
815 *transport)*. Tech. rept. LUBW.

816 LUBW (2006b) *Projet INTERREG III Monit : Structure hydrogéologique et caractéristiques*
817 *hydrauliques (INTERREG III project Monit : Hydrogeological structure and hydraulic*
818 *characteristics)*. Tech. rept. LUBW.

819 Majdalani S, Ackerer P (2010) Identification of Groundwater Parameters Using an Adaptive
820 Multiscale Method. Application to the Upper Rhine aquifer. *Groundwater*, no. doi:
821 10.1111/j.1745-6584.2010.00750.x.

822 Nash J E, Sutcliffe J V (1970) River flow forecasting through conceptual models, 1 : A
823 discussion of principles. *Journal of Hydrology*, **10**, 282–290.

824 Noyer M L, Elsass P (2006) Modelling aquifer salinity in the Potash Basin (Alsace). In:
825 *International Symposium on Aquifer Systems Management - 30th May - 1st June*
826 *2006, Dijon, France*.

827 Philippe E, Habets F, Ledoux E, Goblet P, Viennot P, Mary B (2010) Improvement of the
828 solute transfer in a conceptual unsaturated zone scheme: a case study of the Seine
829 River Basin. *Hydrological Processes*, **In press**.

830 PIREN-Eau-Alsace (1984) *Recherche methodologique sur les hydrosystemes pour optimiser*
831 *la gestion des ressources en eau dans la region Alsace (Methodologic research on*
832 *hydrosystems to optimize water resources management in the Alsace region)*. Tech.
833 rept. Région Alsace.

834 Quintana-Segui P, LeMoigne P, Durand Y, Martin E, Habets F, Baillon M, Canellas C,
835 Franchisteguy L, Morel S (2008) Analysis of Near-Surface Atmospheric Variables :
836 Validation of the SAFRAN analysis over France. *Journal of Applied Meteorology and*
837 *Climatology*, **47**, 92–107.

838 Refsgaard J C (1997) Parameterisation, calibration and validation of distributed hydrological
839 models. *Journal of Hydrology*, **198**, 69–97.

840 Rushton K (2007) Representation in regional models of saturated river-aquifer interaction for
841 gaining/losing rivers. *Journal of Hydrology*, **334**(1-2), 262 – 281.

842 Sanford W. (2002) Recharge and groundwater models: an overview. *Hydrogeology Journal*,
843 **10**, 110-120.

844 Schmitt L (2001) *Typologie hydro-geomorphologique fonctionnelle de cours d'eau :
845 recherche methodologique appliquee aux systemes fluviaux d'Alsace (Hydro-
846 geomorphologic fonctionnal typology of streams : methodologic research applied to
847 the fluvial systems in Alsace)*. Ph.D. thesis, Universite Louis Pasteur, Strasbourg.

848 Sophocleous M (2002) Interactions between groundwater and surface water : the state of the
849 science. *Hydrogeology Journal*, **10**, 52–67.

850 Therrien, R., McLaren, R. G., Sudicky, E. A., & Panday, S. M. 2007. *HydroGeoSphere: A
851 Three-dimensional Numerical Model Describing Fully-integrated Subsurface and
852 Surface Flow and Solute Transport*. Tech. rept.

853 Vidal, Jean-Philippe, Martin, Eric, Franchistéguy, Laurent, Baillon, Martine, & Soubeyroux,
854 Jean-Michel. 2009. A 50-year high-resolution atmospheric reanalysis over France with
855 the Safran system. *International Journal of Climatology*.

856 Wilks D S (1995) *Statistical Methods in the Atmospheric Sciences*. Elsevier.

857 Woessner W W (2000) Stream and Fluvial Plain Groundwater Interactions : Rescaling
858 Hydrogeologic Thought. *Groundwater*, **38**, 423–429.

Figure1

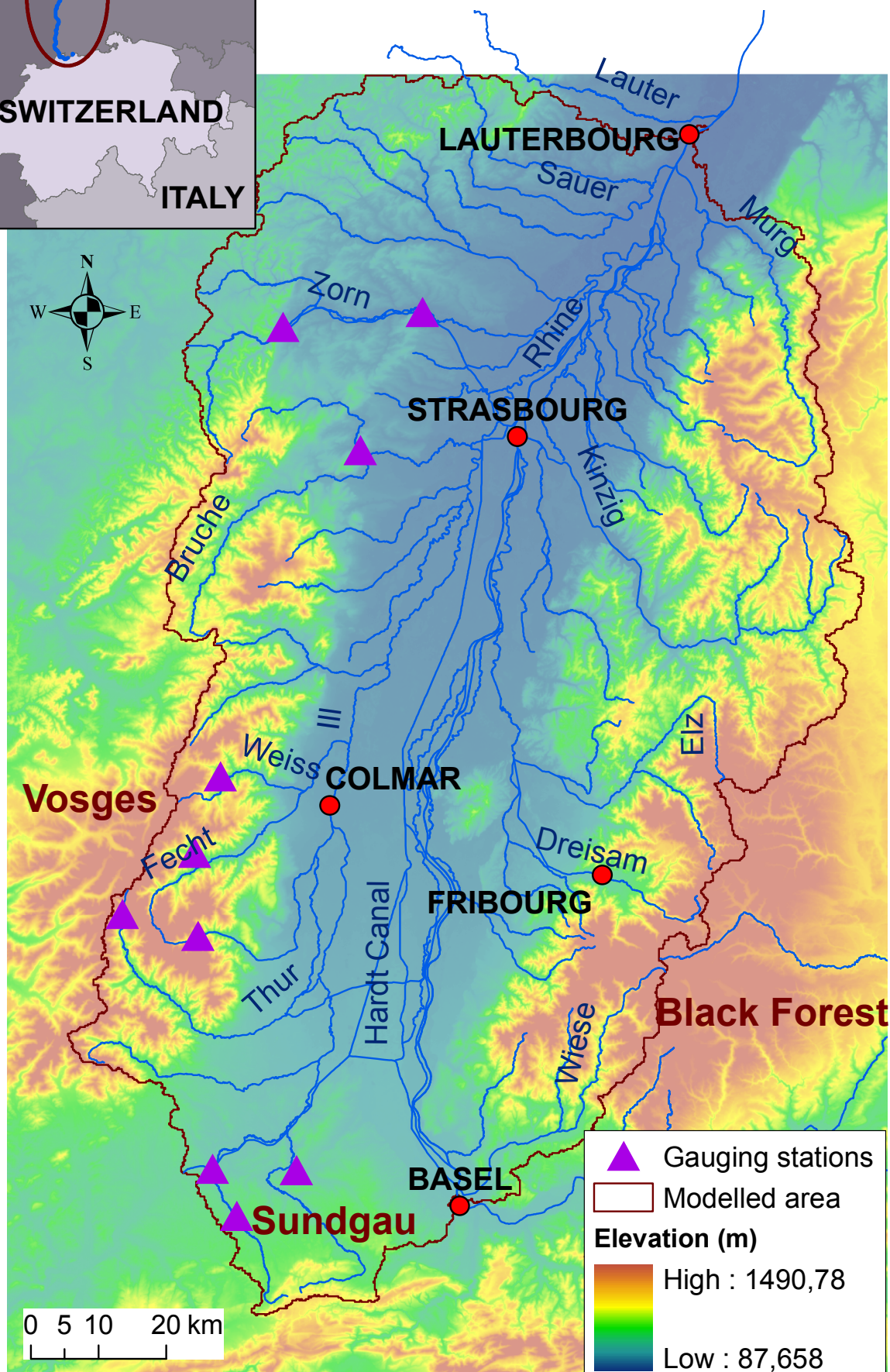
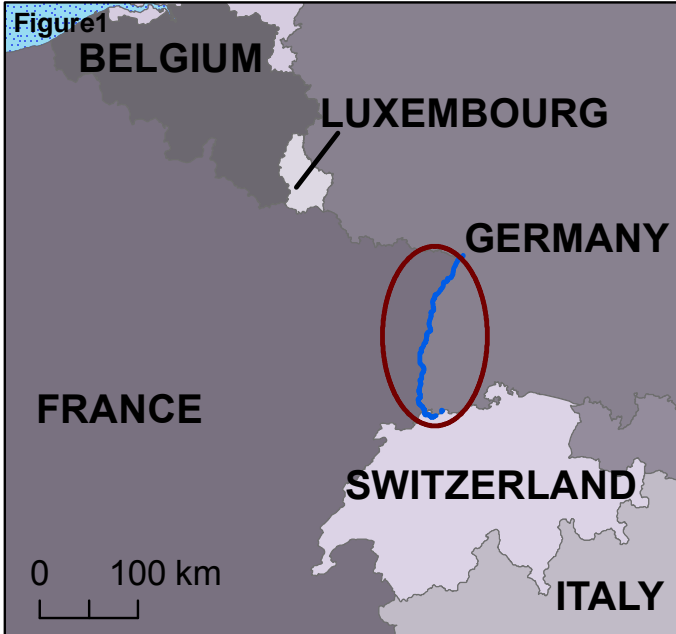


Figure1
[Click here to download high resolution image](#)

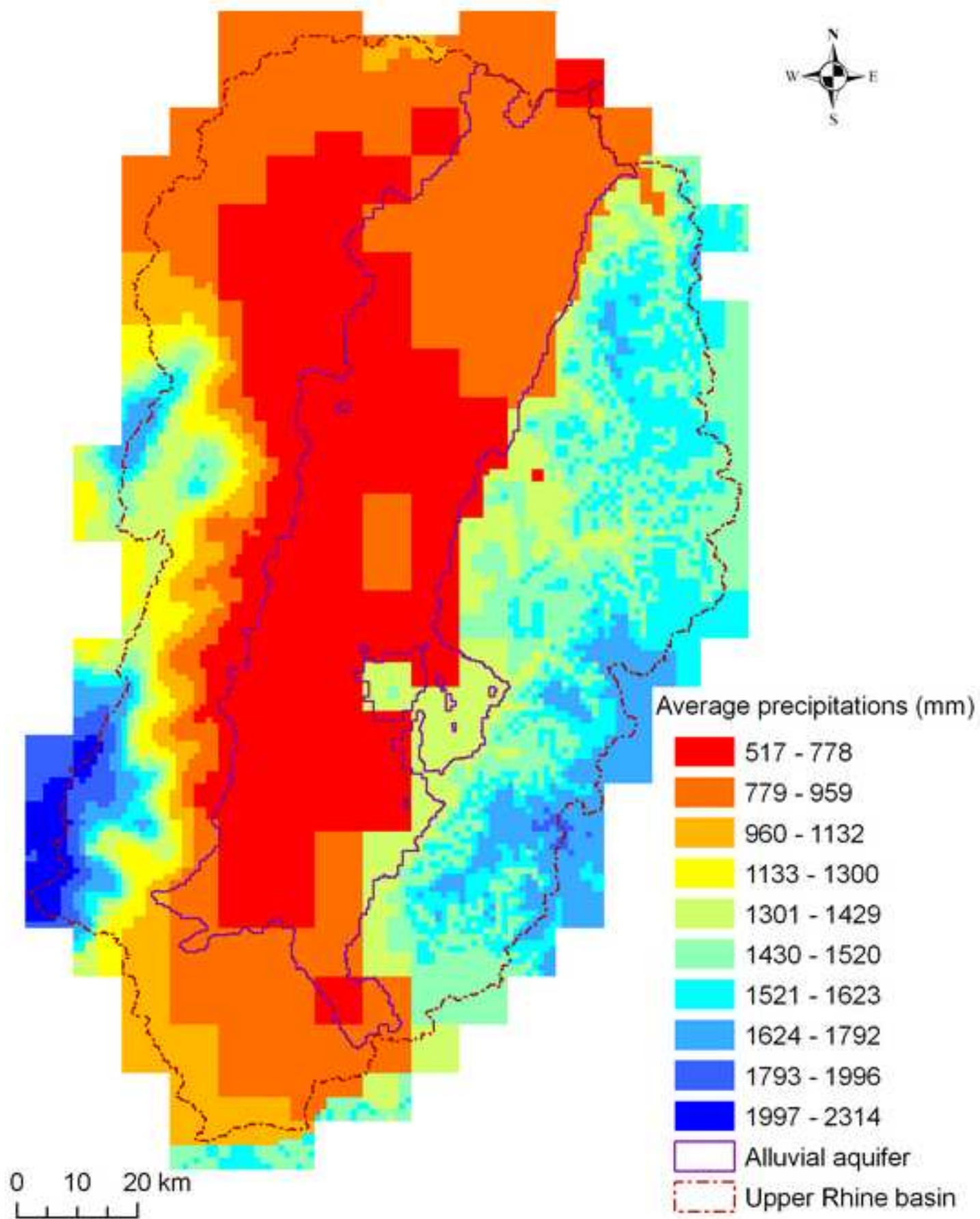


Figure2

[Click here to download high resolution image](#)

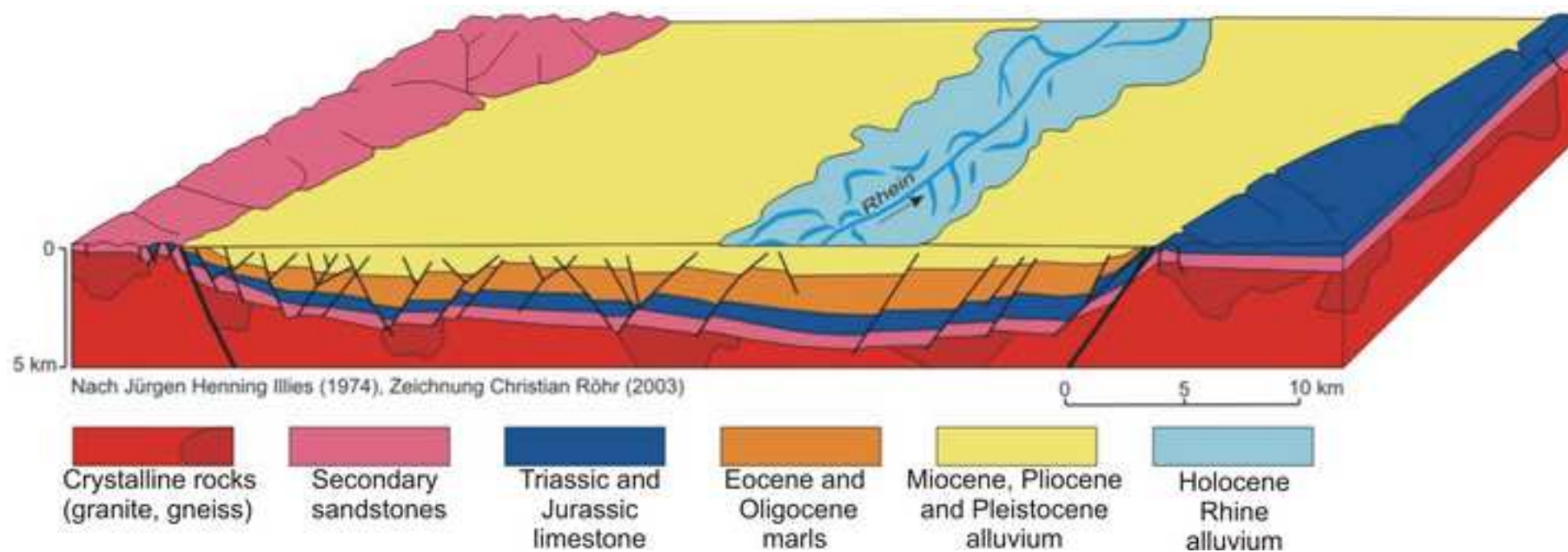


Figure3

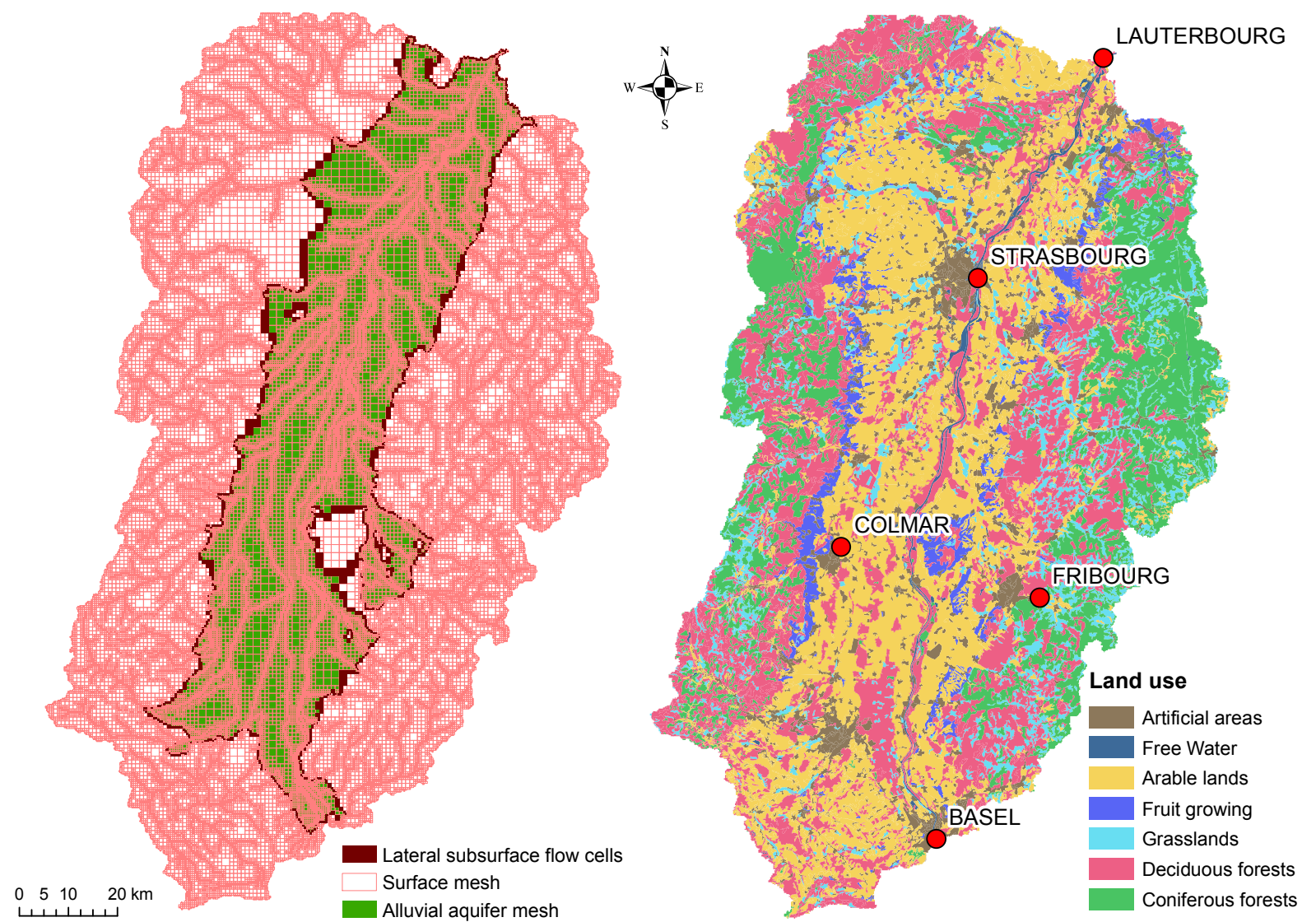


Figure4

[Click here to download high resolution image](#)

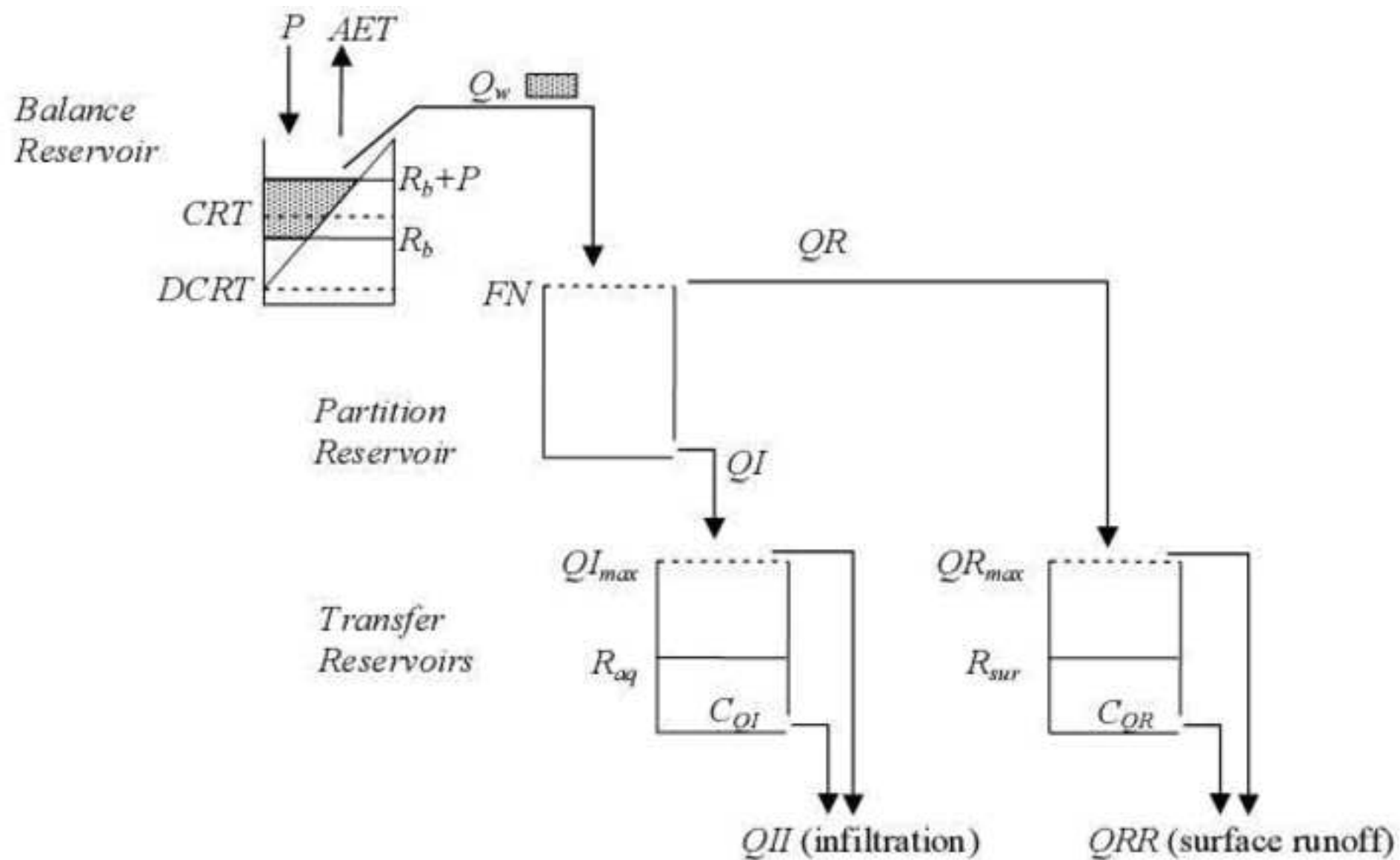
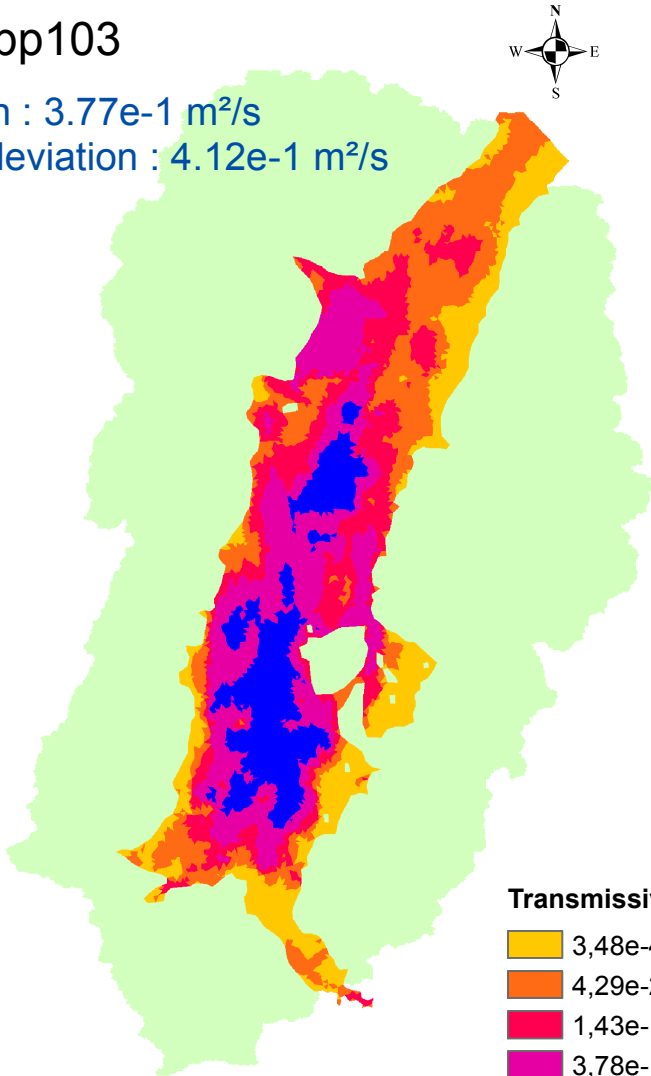


Figure5

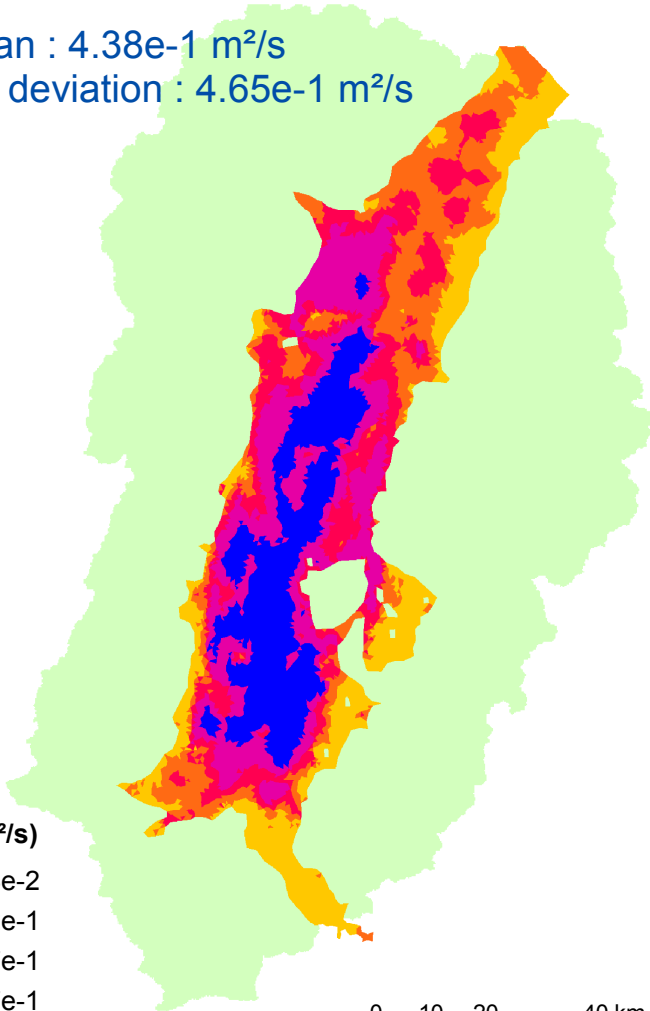
T hpp103

Mean : $3.77\text{e-}1 \text{ m}^2/\text{s}$
Std deviation : $4.12\text{e-}1 \text{ m}^2/\text{s}$



T hpp47

Mean : $4.38\text{e-}1 \text{ m}^2/\text{s}$
Std deviation : $4.65\text{e-}1 \text{ m}^2/\text{s}$



Transmissivity (m^2/s)

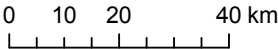
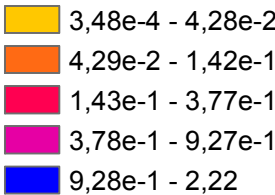
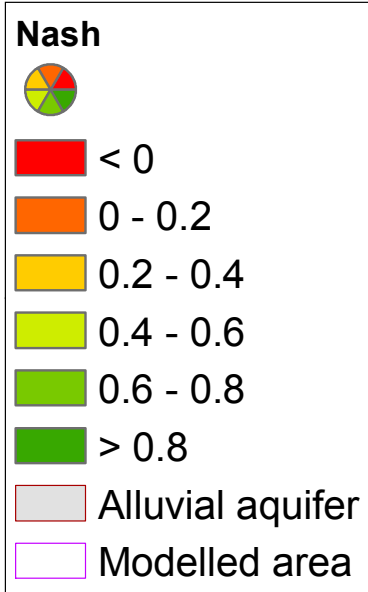
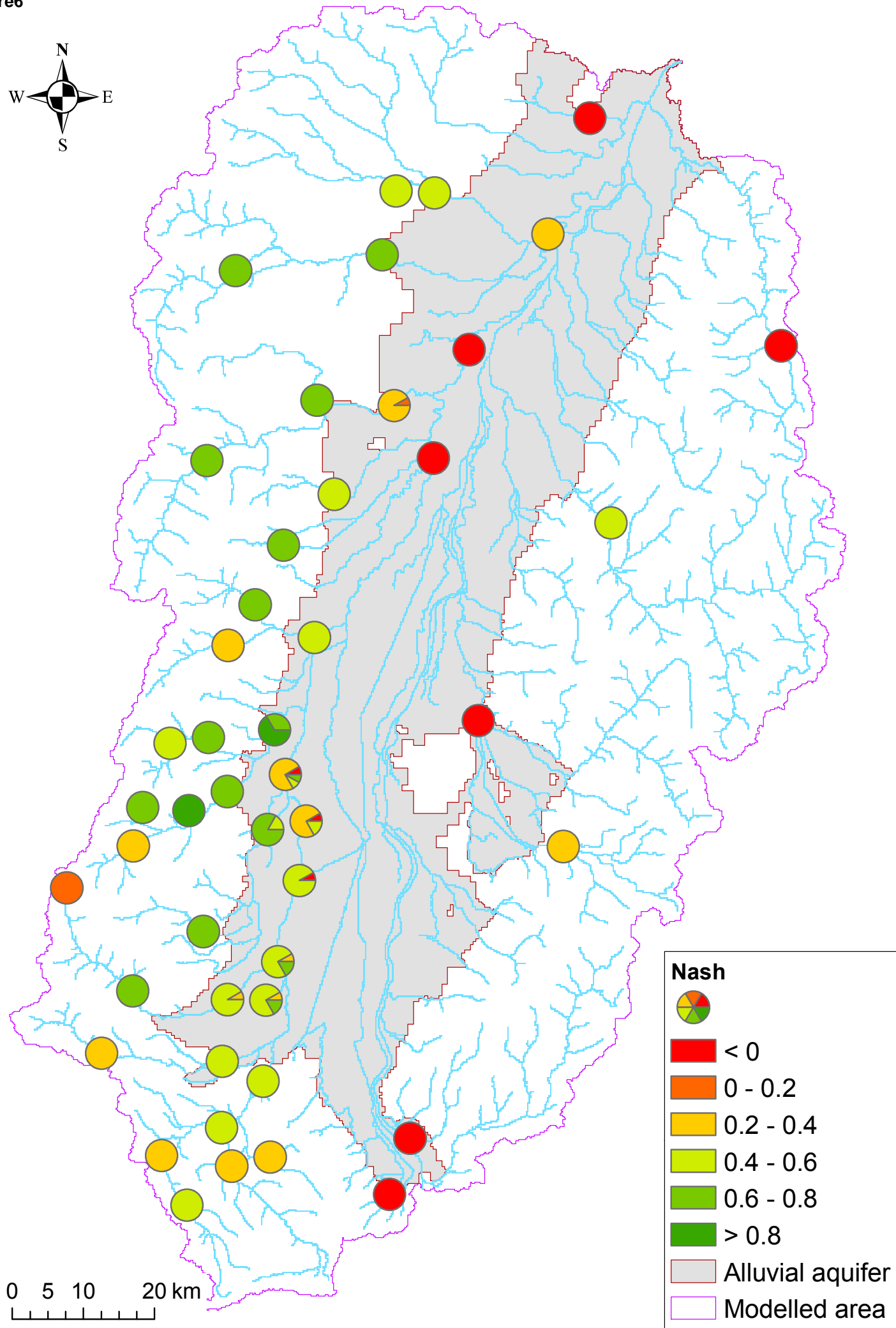
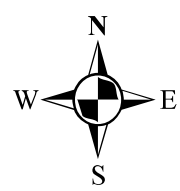
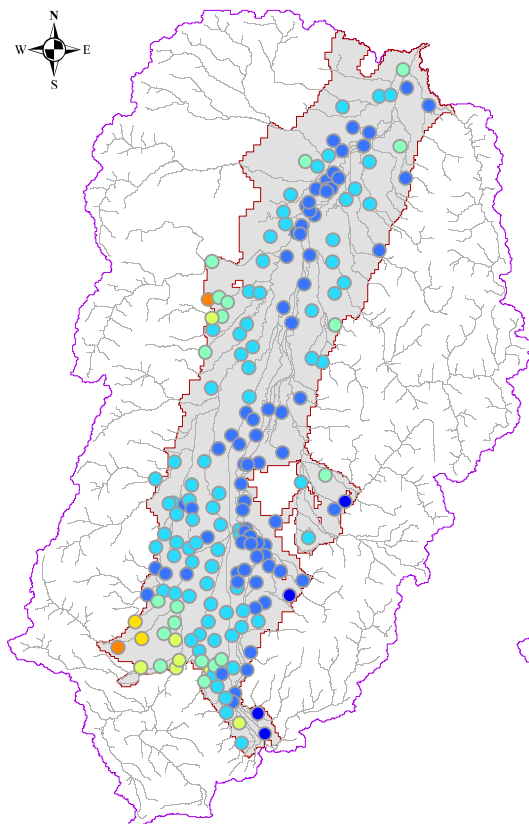
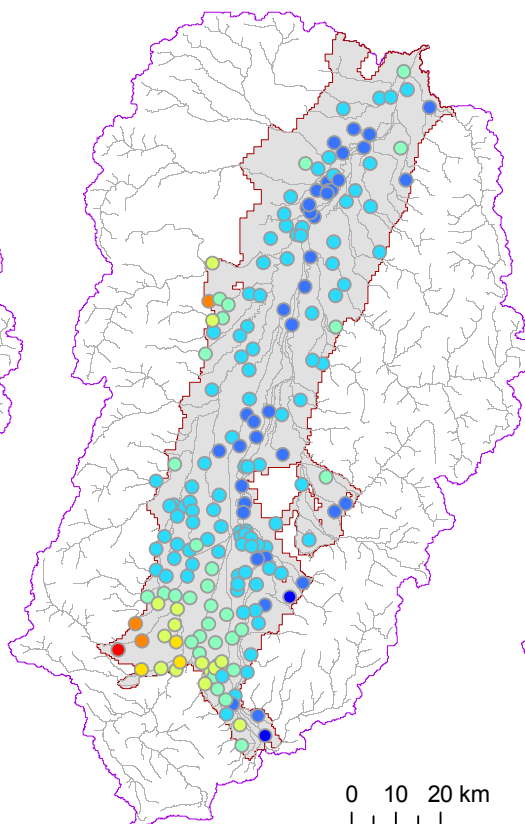


Figure6

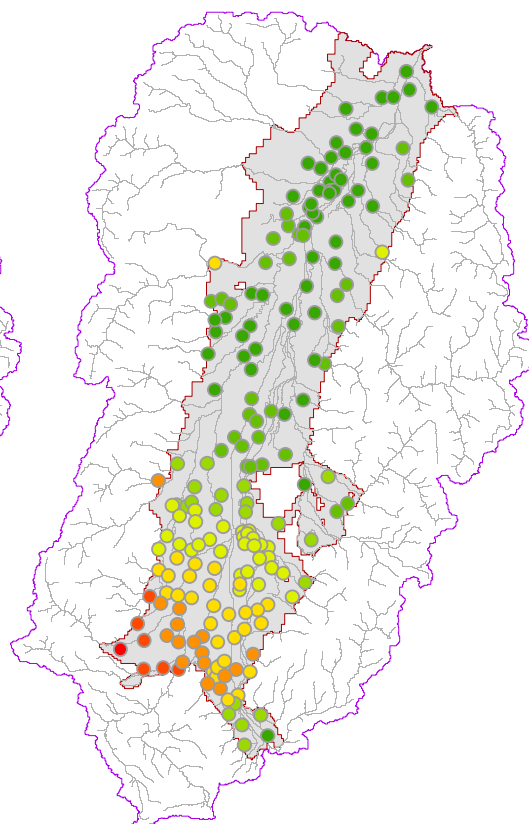




Mean values for the 12 simulations



Standard deviation over the 12 simulations



0 10 20 km

Figure8

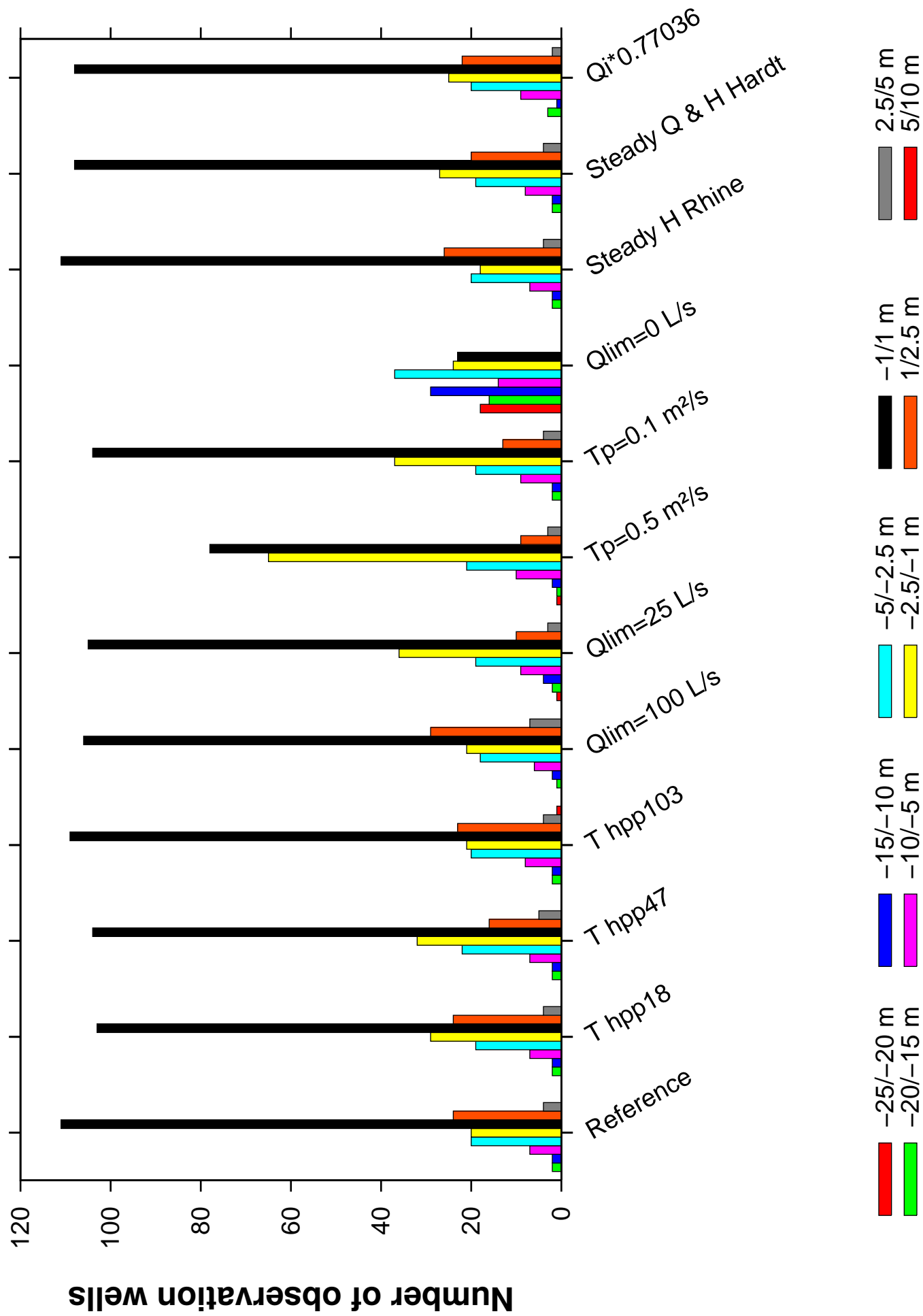


Figure9
[Click here to download high resolution image](#)

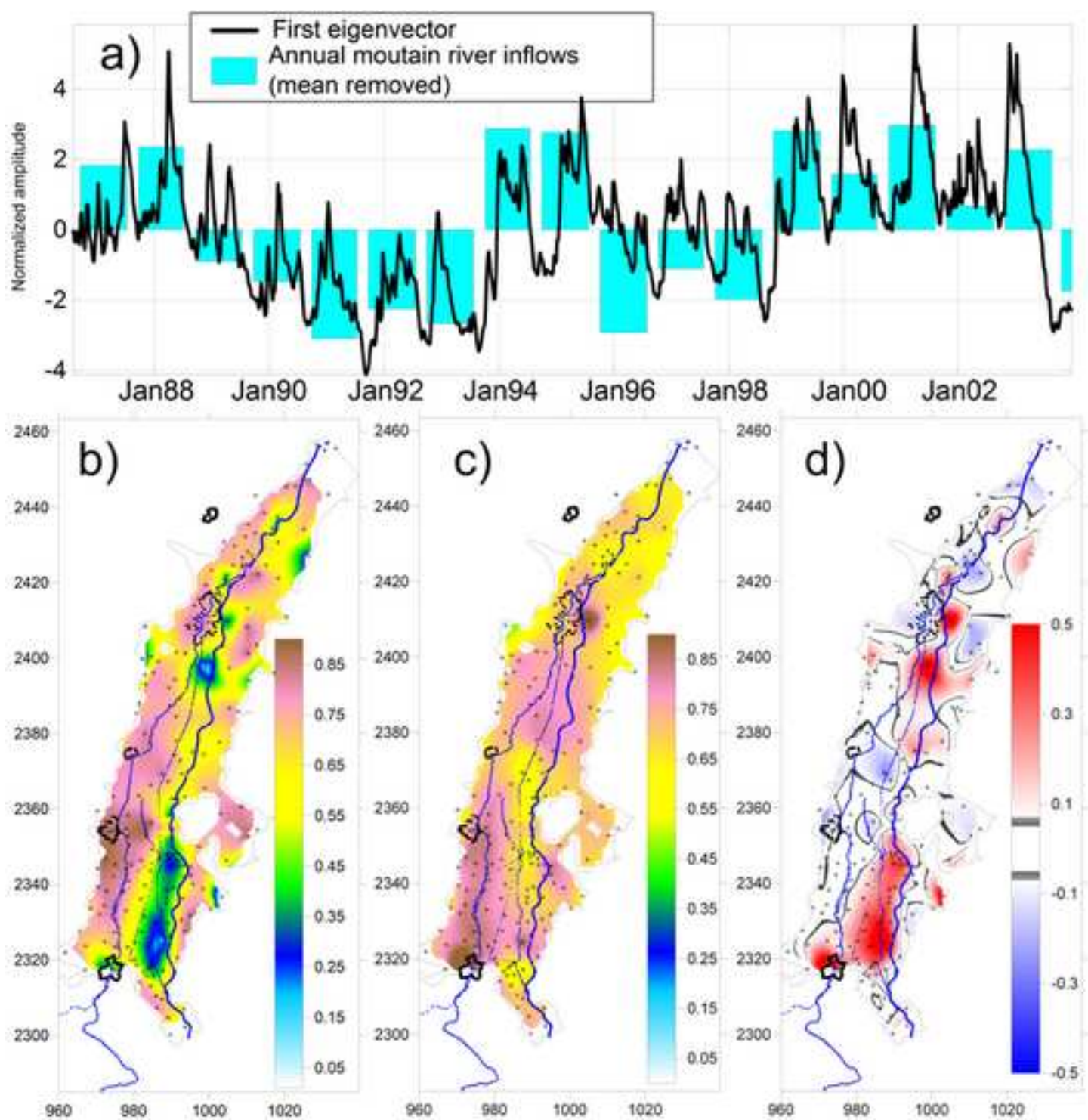


Figure10

[Click here to download high resolution image](#)

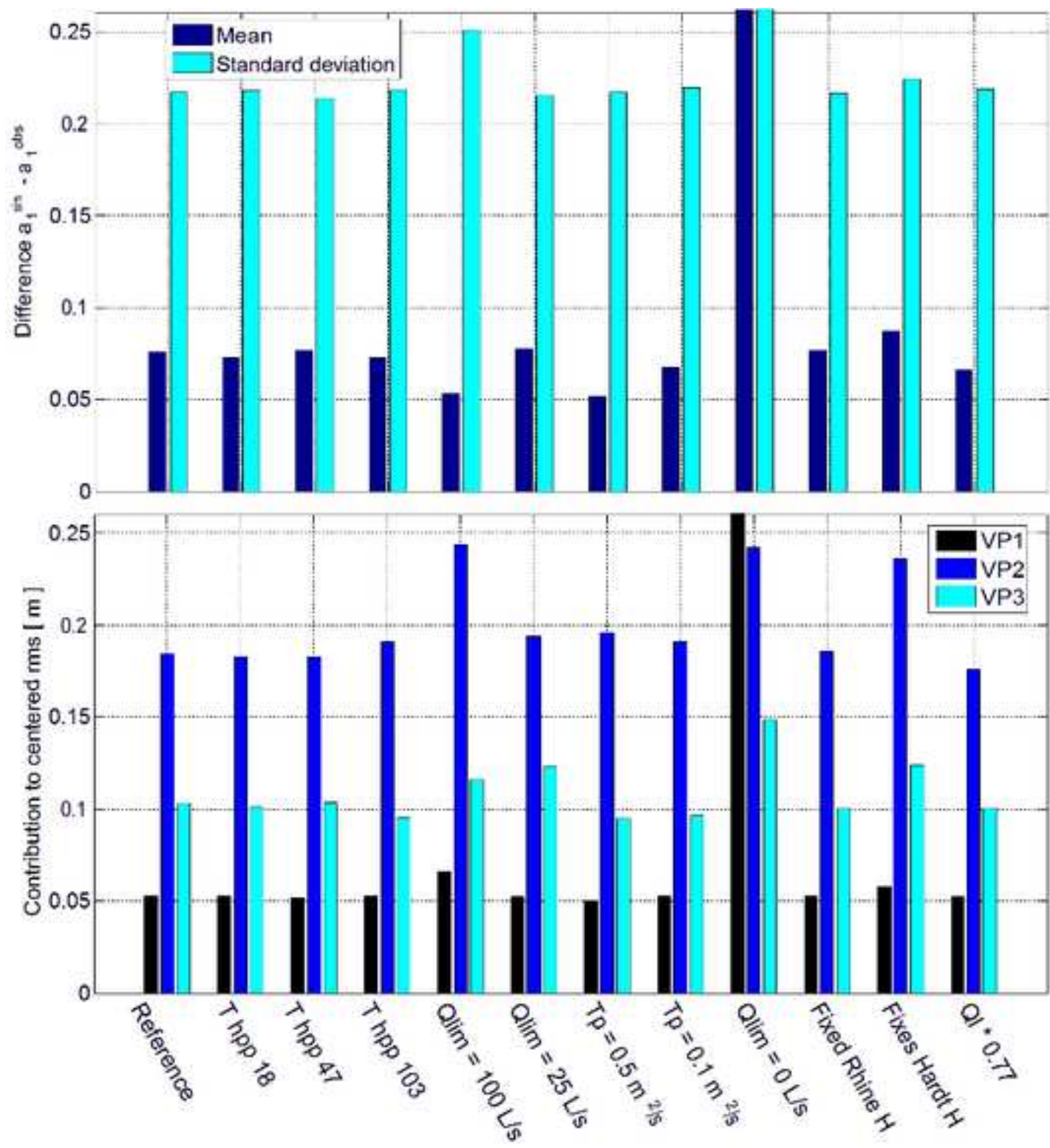


Figure11

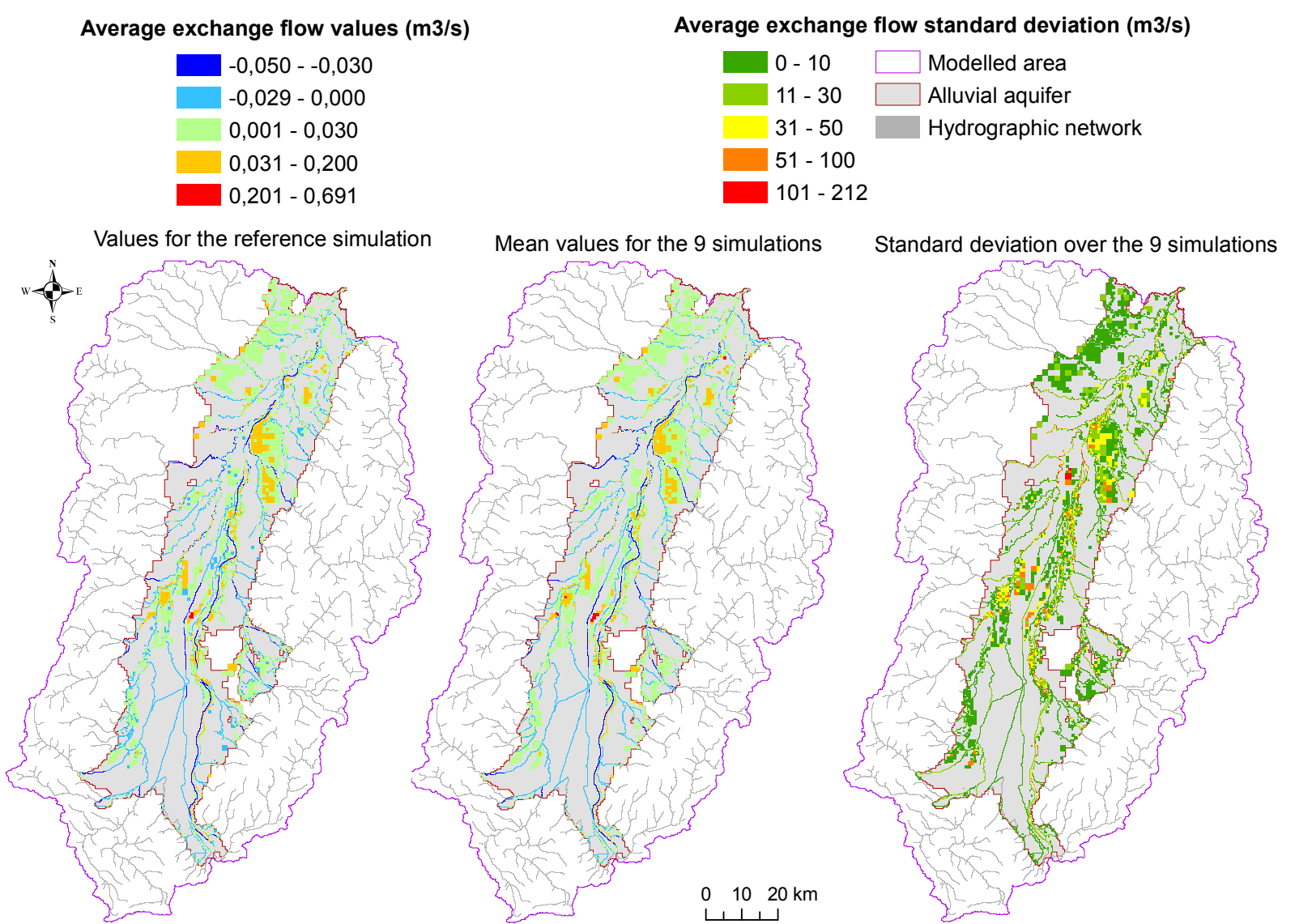


Figure12

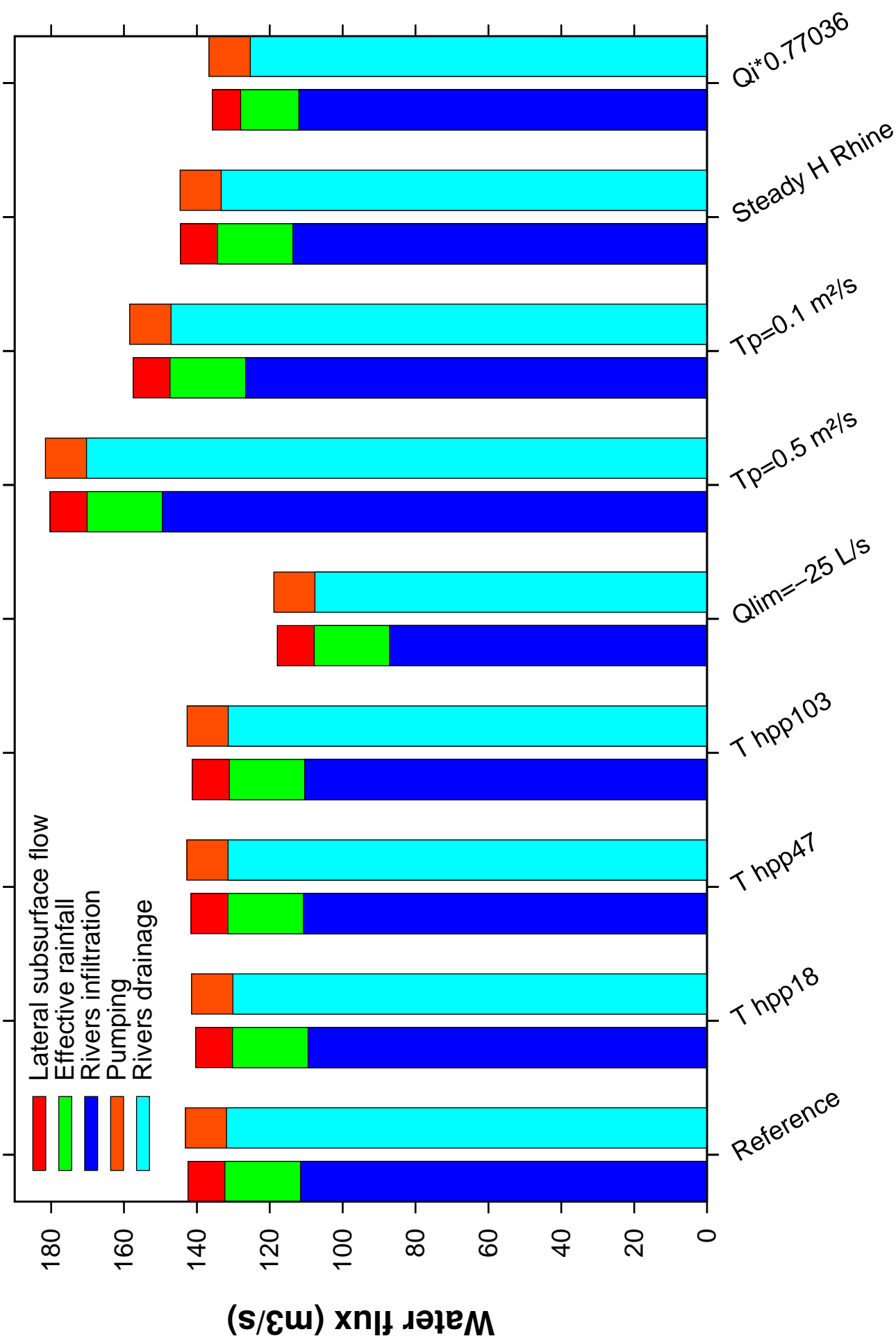


Figure13

